Swiss Soft Days

15th Edition
Ecole Polytechnique Fédérale Lausanne

Thursday, October 2nd 2014

Program
&
Abstracts

Swiss Soft Days XV

EPFL, Lausanne – Cubotron, Auditorium 1
2nd October 2014, 9:00 to 17:30

9:00 – 9:45	Registration and coffee	
9:45 – 10:00	Introduction and welcome	Paolo De Los Rios (EPFL)

10:00 – 11:00	Session I: Biological systems	
10:00 – 10:15	Lipid self-assembly and its applications in biomedical engineering	K. Sugihara (Univ. Geneva)
10:15 – 10:30	Rheology of extracellular matrices of swarming colonies of *P. aeruginosa.*	R. De Dier (ETHZ)
10:30 – 10:45	DNA in confined geometry.	A. Japaridze (EPFL)
10:45 – 11:00	Controlling Enzymatic Activity and Kinetics in Swollen Mesophases by Physical Nano Confinement	W. Sun (ETHZ)

11:00 – 11:30	Coffee break and Poster session

11:30 – 12:15	Session II: Theory	
11:30 – 11:45	Microrheology close to an equilibrium phase transition	A. Scacchi (Univ. Fribourg)
11:45 – 12:00	Hydrodynamic interactions of two nearly-touching Brownian spheres	M. Radiom (Univ. Geneva)
12:00 – 12:15	Structure of marginally jammed polydisperse packings of frictionless spheres	C. Zhang (Univ. Fribourg)

12:15 – 14:00	Lunch break

14:00 – 14:45	Session III: Environmental sensing	
14:00 – 14:15	Size-dependent deswelling of pNIPAM microgels in binary suspensions	A.Scotti (PSI)
14:15 – 14:30	Encapsulation of temperature sensitive manterials by environamentally controlled emulsion electro-spinning	A. Camerlo (Univ. Geneva)
14:30 – 14:45	Optically responsive supramolecular glasses	D. W. R. Balkenende (Univ. Fribourg)

14:45 – 15:45	Invited talk: Disordered actomyosin contracts in unexpected ways	M. Lenz (Univ. Paris-Sud)

Swiss Soft Days XV

15:45 – 16:15	Coffee break and Poster session

16:15 – 17:15	Session IV: Self assembly	Chair:
16:15 – 16:15	High frequency microrheology of enantiomeric peptide hydrogel networks	P.J. Beltramo (ETHZ)
16:30 – 16:30	Polymer dynamics in self-assembled block copolymer membranes	F. Itel (Univ. Basel)
16:45 – 17:00	Structured Device Materials By Polymer Self Assembly	U. Steiner (Adolphe Merkle Institute)
17:00 – 17:15	Scanning Tunneling Microscopy characterization of gold nanoparticles: morphologies of the ligand shell	Q. Ong (EPFL)

17:15 – 17:30	Conclusions and announcement of SSD 16

Swiss Soft Days XV

How to reach the Cubotron, EPFL

How to reach EPFL by public transport

The fastest way is to take a train to "Renens VD", then take the subway 'M1' (Direction: Lausanne-Flon) and get off at the ‘UNIL Sorge’ stop.

Alternatively, you can take a train to Lausanne Gare, then take the subway ‘M2’ (Direction: Croisettes) to ‘Lausanne-Flon’. There take the subway ‘M1’ (Direction: Renens Gare) and get off at the ‘UNIL Sorge’ stop.

You will get all the information (timetable, connections) on the Swiss Railway site (type "UNIL Sorge" as destination). The Cubotron building is then on your right.

How to reach EPFL by car

Motorway A1 direction Lausanne-Sud, take the exit "UNIL-EPFL". Follow the 'Route du Lac' ('Route Cantonale') along the lake to the EPFL campus. You can also set your GPS to the crossing between Av. Forel and R. de la Sorge in Ecublens.

Abstracts for the short talks

Swiss Soft Days XV

Lipid self-assembly and its applications in biomedical engineering

K. Sugihara

University of Geneva, Geneva, Switzerland.

INTRODUCTION: Biological nanofabrication by self-assembly is the sustainable technology that could potentially inspire and supplement the conventional clean-room-based lithography techniques. Our lab, which started at the University of Geneva from April 2014, focuses on studying the mechanism of lipid self-assembly and develops applications in the field of biomedical engineering.

RESULTS: Previously we have discovered that the main component of bacterial cell membranes, 1,2-dioleoyl-sn-glycero-3-phosphoethanolamine (DOPE), self-assembles into single-wall nanotubes.[1] The lipid nanotubes (LNT) were visualized by fluorescence microscopy and transmission electron microscopy. The diameter of the tube is 20 nm and they can be patterned on surfaces either by microfluidic systems or by micromanipulators. We also study the transformation of vesicles into supported lipid bilayers (*i.e.* planar lipid bilayers on solid surfaces, SLB) because there is a demand to develop versatile SLB formation techniques for membrane protein studies. We have demonstrated several tricks to form SLBs with many types of lipids on different substrates. For example, the mechanical forces imposed by the ice formation can trigger the rupture of adsorbed vesicles into SLBs.

Such self-assembled lipid structures are tested for the use in different applications. We applied surface-bound self-assembled LNTs as force detectors to visualize the contractile activity of spreading cells.[2] The newly generated LNTs upon cell spreading exhibited fingerprints characteristic for cell types and conditions. The system can be used as a label-free cell toxicity assay since the loss of contractility is an early sign for cell death. SLBs created with developed methods are used for electrophysiology. A SLB was formed over a single 800-nm pore in a Si/Si_3N_4 chip by pre-filling the pore with a polyelectrolyte multilayer (PEM) to enable the spontaneous fusion of 50-nm liposomes over the pore.[3] The single channel activities of the pore-forming peptide melittin were recorded over a period of two and a half weeks. The 200–times longer lifetime of the artificial cell membrane compared to the patch clamp method revealed a new feature of the peptide, the time-dependent stabilization effect upon bias application.

REFERENCES:

1. K. Sugihara, et al., ACS nano **6**, 6626 (2012).
2. K. Sugihara, et al., Integrative biology **5**, 423 (2013).
3. K. Sugihara, et al., ACS nano **4**, 5047 (2010).

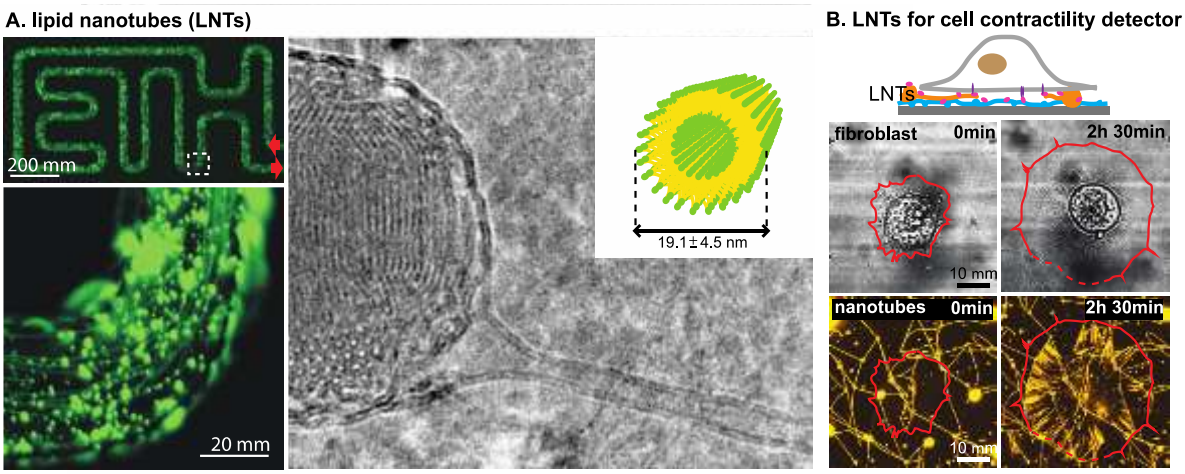

Figure 1 A. Surface-patterned self-assembled lipid nanotubes from inverted hexagonal structures. Fluorescent images (left) and a cryoTEM image (right). B. Label-free detection of cell-contractile activity with lipid nanotubes. Images extracted from a time-lapse of rat embryo fibroblast (REF52) cells spreading on a glass surface coated with lipid nanotubes. Bright field images of REF cells (upper) and fluorescent images of the lipid nanotubes underneath the cell (lower).

Rheology of extracellular matrices of swarming colonies of *P. aeruginosa*

Raf De Dier[1,2], Jan Vermant[1]

[1] ETH Zürich, Zürich, Switzerland. [2] University of Leuven, Leuven, Belgium.

INTRODUCTION: Bacterial colonies of *Pseudomonas aeruginosa*, a pathogenic organism, exhibit complex swarming and spreading phenomena, used by these microorganisms when invading and colonising solid surfaces[1]. The bacteria live in an extracelullar matrix composed of polysaccharides, DNA fragments and other secreted products. The rheology of this matrix plays an important role for both the motion of the individual bacteria as well as for the collective swarming behaviour. In the present work we characterise the rheological response of this matrix, using both macroscopic bulk rheology and passive and active microrheological techniques. The rheological properties on both the local scale motion and the macroscopic swarming behaviour show large discrepancies and may provide insight in the structuring of the biofilm and its influence on the colonizing behaviour of the bacterial colony.

METHODS: *Pseudomonas aeuginosa* biofilms were cultivated and grown in swarming condition, as to obtain a densely populated biofilm. Initial inoculation in liquid LB media overnight at 37°C (5% CO2), was subsequently grown on adjusted 0,5% agar-agar plate and allowed to swarm over a timescale of 14h. Careful harvesting of the swarmed biofilm allowed rheological investigation. A custom-made high speed confocal setup (VisiTech, UK) was used to perform microrheological experiments. Passive Brownian motion allowed measuring the frequency response of the bacterial biofilm on the local microscale. A self-built magnetic tweezer setup using strong electromagnets could mimic the active motion of individual bacteria within the extracellular matrix. An AR-G2 (TA Instruments, USA) was used to perform macroscopic bulk rheological measurements.

RESULTS & DISCUSSION: Figure 1 shows the macroscopic bulk rheological response on a stress-controlled rheometer of the extracellular matrix of *Pseudomonas aeruginosa*, where a high biofilm viscosity value is found for both low and medium shear rates. In light of the force an individual bacterium can exert while swimming in liquid medium, it would be expected that these organisms would travel at very low speeds, which would be detrimental for their translocation and surface colonisation. However, using confocal microscopy, high velocities up to 20 µm/s were witnessed during live swarming. These observations reveal that a large discrepancy may exist between the rheological properties of the biofilm and the microscale properties.

Using the passive, Brownian motion of particles of the same size as the *P. aeruginosa* cells, a heterogeneous response of the biofilm was measured on the microscale, where in total 5 distinct regions were revealed. Within these regions, the individual bacteria used the low-viscous pathways in order to move within the matrix in a fast way. In contrast, the elastic regions contributed to the overall macroscopic strength of the biofilm to withstand external stresses.

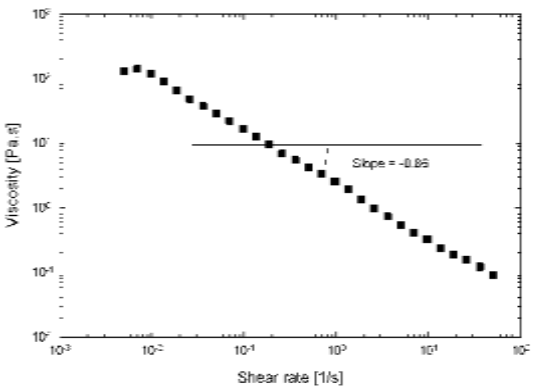

Fig. 1: Macroscopic viscosity curve as function of shear rate for the extracellular matrix of Pseudomonas aeruginosa.

REFERENCES: [1] Fauvart et al.; **2012**; *Soft Matter; 8:70-76* [2] Sempels et al.; **2013**; *Nat. Commun.; 4: 1757*

ACKNOWLEDGEMENTS: This work was supported by a research fellowship of the FWO-Vlaanderen.

Swiss Soft Days XV

DNA in confined geometry

Aleksandre Japaridze[a], Kathleen Smith[a], Francesco Valle[b] and Giovanni Dietler[a],

a Laboratoire de Physique de la Matière Vivante, Ecole Polytechnique Fédérale de Lausanne, CH-1015 Lausanne,Switzerland

b Institute of Nanostructured Materials-CNR, Bologna, Italy

INTRODUCTION: DNA is a very important object of study for geneticists and biologists as well as for physicist. It is important to understand the role of topology of DNA in confined geometry, to better understand such processes as DNA migration in nanofluidics devices or DNA compaction in Viral capsids.

METHODS: Here we present a novel experimental method for studying effects of geometrical confinement on DNA molecules. The confinement is created by letting a DNA solution diffuse into PDMS slits placed on a mica surface. By combining a Microfluidics device with Atomic Force Microscopy technique we are able to directly visualize and measure the effects of confining space (in z dimension) on the statistical parameters of a non-stained DNA.

RESULTS: We tested three different types of circular DNA of various sizes (ranging from 2.7kb to 5.4kb) and observed an increase in persistence length and critical exponent for the two biggest circular DNA confined in 140nm slits. Due to the very high spatial resolution of AFM, we were able to directly visualize the change in shape parameters and morphology of DNA upon mild confinement.

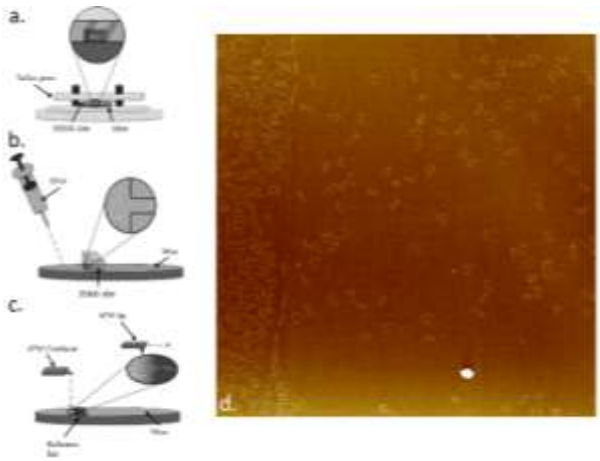

Fig. 1: a .Schematic representation of the Teflon clamp where the microfluidics slits are gently pressed on the surface; b Schematic representation of sample deposition and the zoomed image showing the translocation of circular DNA inside slits; c. Schematic representation of an AFM tip scanning the mica surface d. A typical AFM image showing circular pUC19 (2686bp) DNA migrating into giant slits. The orientation of the slit entrance is left to right.

DISCUSSION & CONCLUSIONS: This new approach had several improvements compared to experimental procedures previously reported: it had a significantly higher spatial resolution (based off AFM resolution), it enabled us to control the height of the confinement with very high precision and there was no need to stain the DNA for experiments.

Controlling Enzymatic Activity and Kinetics in Swollen Mesophases by Physical Nano-Confinement

*Wenjie Sun, Jijo J. Vallooran, Alexandru Zabara, Raffaele Mezzenga**

Food and Soft Materials Science, Institute of Food, Nutrition & Health, Department of Health Science and Technology, ETH Zürich, Zürich, Switzerland.

INTRODUCTION: Bicontinuous lipid cubic mesophases are widely investigated as hosting matrices for functional enzymes to build biosensors and bio-devices due to their unique structural characteristics. However, the enzymatic activity within standard mesophases (*in-meso)* is severely hindered by the relatively small diameter of the mesophase aqueous channels, which provide only limited space for enzymes, and restrict them into a highly confined environment. We show that the enzymatic activity of a model enzyme, Horseradish Peroxidase (HRP), can be accurately controlled by relaxing its confinement within the cubic phases' water channels, when the aqueous channel diameters are systematically swollen with varying amount of hydration-enhancing sugar ester.

The *in-meso* activity and kinetics of HRP is then systematically investigated by UV-vis spectroscopy, as a function of the size of aqueous mesophase channels. The enzymatic activity of HRP increases with the swelling of the water channels. In swollen mesophases with water channel diameter larger than HRP size, the enzymatic activity is more than double than that measured in standard mesophases, approaching again the enzymatic activity of free HRP in bulk water. We also show that the physically-entrapped enzymes in the mesophases exhibit a restricted-diffusion-induced initial lag period and report the first observation of *in-meso* enzymatic kinetics significantly deviating from the normal Michaelis-Menten behavior observed in free solutions, with deviations vanishing when enzyme confinement is released by swelling the mesophase.

RESULTS: The initial rate of reaction increases exponentially while the relative activity increases linearly with increasing water channel sizes.

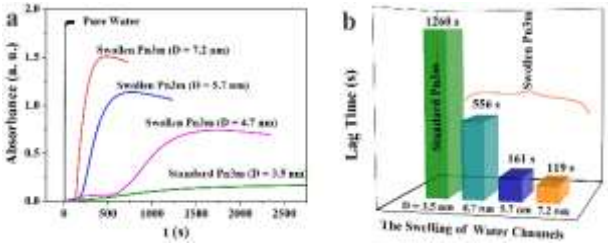

Fig 1. UV progress curves of the enzymatic reaction (a) and lag time (b) within the 4 Pn3m phases with increasing water channels

DISCUSSION & CONCLUSIONS:

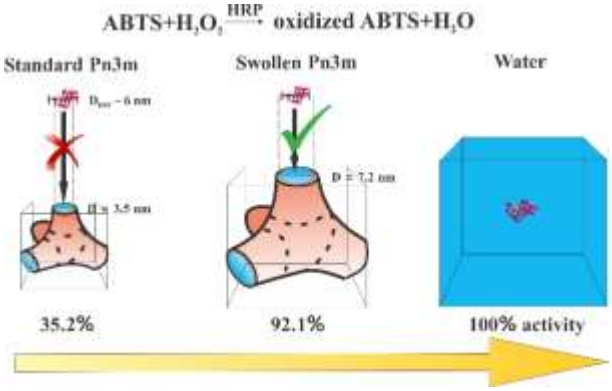

Figure 2. Schemetic illustration of HRP in standard and swollen mesophase.

REFERENCES: E. Nazaruk, R. Bilewicz, G. Lindblom and B. Lindholm-Sethson, Anal Bioanal Chem., 2008, 391, 1569–1578.

ACKNOWLEDGEMENTS: Dr. Renata Negrini (ETH Zürich) is kindly acknowledged for valuable discussions on the swollen mesophase phase behaviors.

MICRORHEOLOGY CLOSE TO AN EQUILIBRIUM PHASE TRANSITION

J. Reinhardt[1], A. Scacchi[1], J.M. Brader[1]

[1] *University of Fribourg, Fribourg, Switzerland.*

INTRODUCTION: We investigate the microstructural and microrheological response to a tracer particle of a two-dimensional colloidal suspension under thermodynamic conditions close to a liquid-gas phase boundary. On the liquid side of the binodal, increasing the velocity of the (repulsive) tracer leads to the development of a pronounced cavitation bubble, within which the concentration of colloidal particles is strongly depleted. The tendency of the liquid to cavitate is characterized by a dimensionless "colloidal cavitation" number. On the gas side of the binodal, a pulled (attractive) tracer leaves behind it an extended trail of colloidal liquid, arising from downstream advection of a wetting layer on its surface. For both situations the velocity dependent friction is calculated.

METHODS: The methods we use to solve these problems are the classical Density Functional Theory (DFT) and the classical Dynamical Functional Theory (DDFT).

RESULTS: For an hard tracer, in the Figure 1, one can see different state points of the phase diagram, for different flux velocity. The cavitation is evident, when the state point lies close to the the liquid-phase boundary. Figure 2 shows different state points, for an attractive tracer, for different flux velocities. On the gas side of the binodal, the tracer leaves an extended trail of wetting layer.

Fig. 1: Density profiles around a tracer pulled with constant velocity. The bulk volume fraction is 40% and the tracer radius Rt=4r. Bottom row: Profiles for pure hard disks (B=0) and dimensionless tracer velocities v=0, 0.1, 0.2. Middle row: Profiles for intermediate attraction strenght (B=6.25) at the same three values of v. Top row: Profiles for a statepoint close to the binodal (B=12.5) illustrating the phenomenon of cavitation.

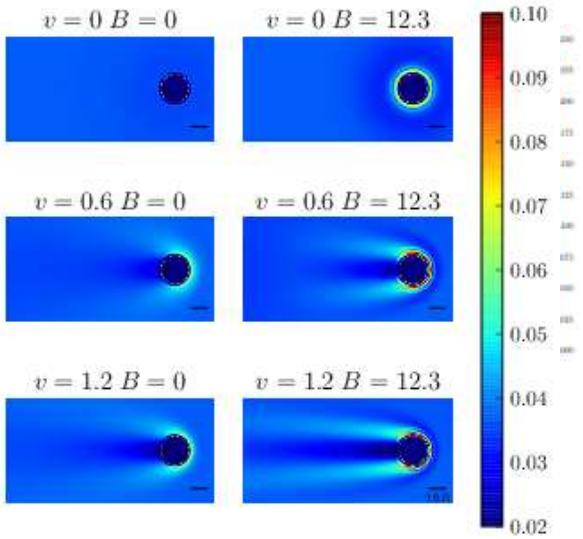

Fig. 2: Density profiles for an attractive tracer, for an occupied volume fraction 11.7%. Left column: pure hard disks (B=0). Right column: square well attraction (B=12.3). The top right panel shows an equilibrium wetting layer, which evolves into an extended wetting trail as the velocity is increased.

DISCUSSION & CONCLUSIONS: Applying DDFT to study the response of the suspension to hard tracer moving with constant velocity we obtain cavitating density profiles, for which a large region of low colloidal volume fraction develops behind the tracer. The tendency of the flow to cavitate increases as the bulk osmotic pressure approaches the vapour pressure and as the velocity of the tracer is increased. When applied to an attractive tracer at a statepoint close to the gas side of the binodal we find that the wetting of the tracer surface interacts in a complex way with the imposed flow field, leading to the generation of long wetting trails.

ACKNOWLEDGEMENTS: We thank V. Trappe for helpful discussions.

Hydrodynamic Interactions of Two Nearly-Touching Brownian Spheres

Milad Radiom[1], William Ducker[2], Mark Paul[2]

[1] *University of Geneva, Geneva, Switzerland.* [2] *Virginia Tech, Blacksburg, USA.*

INTRODUCTION: Flow and stability of colloidal dispersions depend on hydrodynamic interaction of particles. Brownian particles undergo thermal fluctuations at high frequency. Here we discuss whether this high frequency motion means that the frequency-dependent motion of the fluid must be considered for interparticle flow. We conclude that at close-to-contact separations the frequency dependence of the fluid motion does not affect the interaction.

METHODS: A microsphere was glued to distal end of a different AFM cantilever. The vertical separation *D* was varied from a few nano- to tens of micrometers using a piezoelectric drive mechanism (Fig. 1). The thermal fluctuations of the two cantilevers, x_1 and x_2, were measured simultaneously at 1 MHz for 16 s. Then the cross-correlation noise spectrum:

$$G_{12} = \int \left\langle x_1(t)\, x_2(0) \right\rangle e^{i\omega t} dt, \qquad (1)$$

in motion of the spheres was calculated, from which the friction of mutual motions of the two spheres ζ_{12} was obtained (Fig. 2).

RESULTS: An Equation that was derived for steady mutual motion of two spheres:[1]

$$\zeta_{12} = 6\pi\eta a \times F(\rho), \qquad (2)$$

agrees with our experimental data (Fig. 2) despite the fact that our experiments are at high frequency ($f = 4$ kHz). η is viscosity and F is a complex function of $\rho = r/a$.[1]

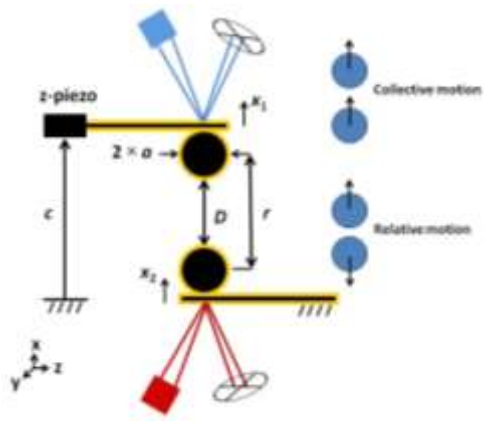

Fig. 1: Schematic of experiment.

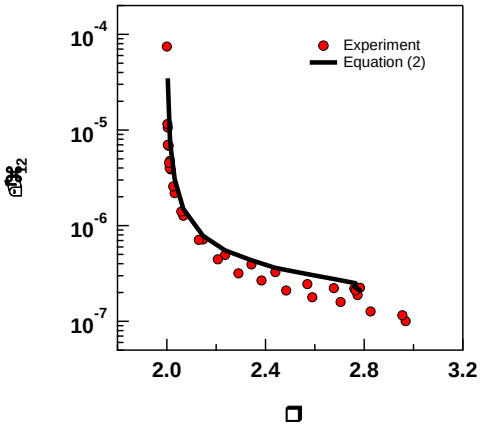

Fig. 2: Friction of mutual motions of two spheres ζ_{12}. *Experiments are in water,* $a = 15$ μm.

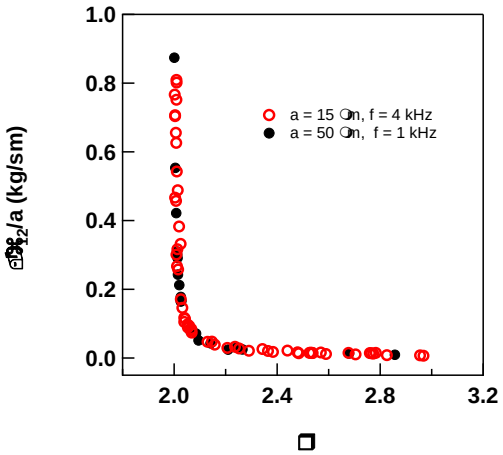

Fig. 3: ζ_{12} *for two oscillation frequencies* f .

DISCUSSION & CONCLUSIONS: Our explanation for the observed agreement between data at high frequency and theory at low frequency (Fig. 2) is that for interparticle gaps *D* shorter than twice the Stokes penetration depth $\sqrt{\upsilon/\pi f}$ where υ is the kinematic viscosity, the interparticle interaction is dominated by flow field in narrow gap between the particles where propagation of stress is effectively instantaneous due to elevated frictional forces. The interparticle interaction is independent of the oscillation frequency f (Fig. 3).

REFERENCES: [1]D.J. Jeffrey; Mathematika;**1982**.

ACKNOWLEDGEMENTS: National Science Foundation of USA.

Structure of marginally jammed polydisperse packings of frictionless spheres

C. Zhang[1], F. Cardinaux[1], T. G. Mason[2], M. Mobius[3], F. Scheffold[1]

1 University of Fribourg, Fribourg, Switzerland.

2 Trinity College Dublin, Dublin, Ireland.

3 University of California, Los Angeles, California, USA.

Using an extended granocentric[1] model (eGCM) we demonstrate how to model the packing structure of a marginally jammed bulk ensemble of polydisperse spheres. We derive a simple relation between the characteristic parameters of the packing, such as the mean number of neighbours and the fraction of rattlers, and the radial distribution function *g(r)*. We find excellent agreement between the model predictions for *g(r)* and computer simulations[2] as well as experiments on jammed emulsion droplets. The observed quantitative agreement opens the pathway towards a full structural characterisation of jammed particle systems for imaging and scattering experiments.

The eGCM divide the particles into two groups: mechanically stable jammed particles and free floating rattlers. We first establish the neighboring shell, taking into account the neighbor-neighbor correlation. The surface-to-surface separation $G_s(s)$ is modelled independently for stable particles and rattlers. We use the scaling of excess number of contacts $Z \sim (Z-Z_J)^{0.5}$ to derive $G_{sJ}(s) \sim s^{-1/2}$. For rattlers we assume their neighbors to be uniformly distributed. Then we adjust the contact to neighbor ratio to reach the isostatic equilibrium. The maximal separation s_{cutoff} is obtained numerically applying the condition $\Phi_J \sim 0.64$ which defines the spatial extension of the first neighboring shell.

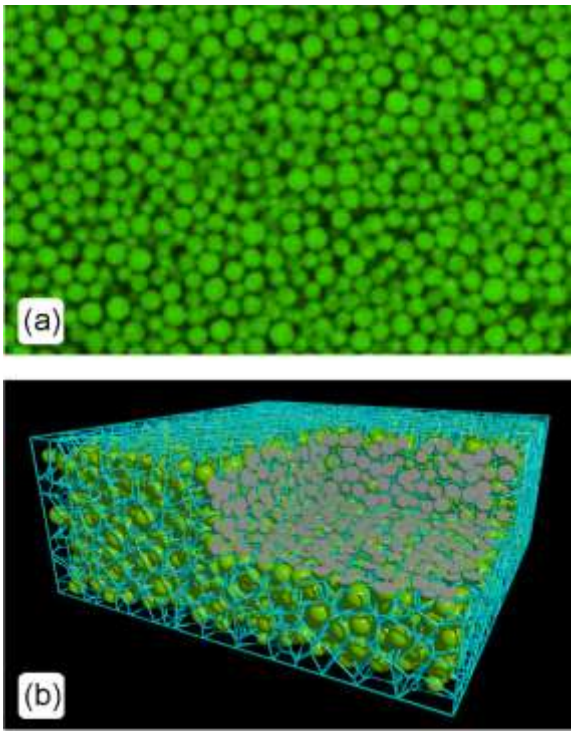

Fig. 1: Three-dimensional imaging of jammed emulsions droplets. (a) Raw image of a plane in the bulk of the sample obtained by laser scanning confocal microscopy of light emitted by the fluorescent dye Nile-red at λ=525nm. The droplets are marginally jammed and the volume fraction is Φ~ 0.64 ± 0.01. (b) Three-dimensional reconstruction of the droplet sizes and positions using the sphere matching method (SMM). The lines show the Voronoi radical tessellation around the droplet centroids. The total dimensions are 51.2μm × 51.2μm × 20.1μm. One corner is cut out to reveal the internal structure of the jammed system.

REFERENCES: *[1] M. Clusel et.al;* ***2009****;* Nature; *460: 611. [2] C. B. O'Donovan et.al;* ***2013****;* Philosophical Magazine; *93: 4030.*

ACKNOWLEDGEMENTS: This project has been financially supported by the Swiss National Science Foundation (Project No. 149867).

Size-dependent deswelling of pNIPAM microgels in binary suspensions

A.Scotti[1,3], U.Gasser[1], E. Herman[2], A. Singh[2], L.A. Lyon[2], A. Fernandez-Nieves[3]

[1] *Laboratory for Neutron Scattering and Imaging – Paul Scherrer Institut, Villigen, Switzerland.* [2] *School of Chemistry and Biochemistry – Georgia Institut of Technology, Atlanta, GA, USA.*
[3] *School of Physics – Georgia Institut of Technology, Atlanta, USA.*

INTRODUCTION: Suspensions of soft microgels with a majority of small particles and a small fraction of big particles with about double size can form crystals without defects caused by the large particles[1]. Due to the softness of microgel, the big particles can shrink to fit into the lattice formed by the small particles.

METHODS: We study the spontaneous deswelling of big particles in a crowed environment of small particles. Fully swollen poly(N-isopropylacrylamide) (pNIPAM) microgel particles have been used. The thermodynamic quantity that rules the phase behavior is the generalized volume fraction ζ. Phase behavior is studied by using series of 10 - 15 samples, which cover the ζ range of interest. Small-angle neutron scattering (SANS), small-angle X-ray scattering (SAXS) and dynamic light scattering are used to characterize the particles and their phase behavior. We observe crystallization in samples with a fraction of big particles n_{big} as high as 0.286.

RESULTS: Using SANS with contrast matching of the small particles, we have shown that the big particles shrink in suspensions with $\zeta \geq 0.6$. We have blended a majority of small, deuterated particles with 10.5% of big protonated ones. The radius of the big particles decreases from 176 nm to 112 nm with increasing concentration as shown in Fig 1. The radius of the small particles was 121nm. The big particles deswell when the osmotic pressure of the suspension is able to compress the fuzzy shell that surrounds the more cross-linked core[2]. With SAXS we have probed the nearest neighbor distance (nnd) in samples with n_{big} increasing from 0.1% up to 80%. At low n_{big}, the nnd of the mixed samples has the same value as the nnd in a sample made of only small monodisperse particles in all the ζ range. Increasing n_{big}, we find a ζ beyond which the nnd is separated from the characteristic value of nnd given by the small monodisperse particles. At higher n_{big}, the nnd of the mixed samples moves away from the value we observe for small particles, towards the value typical for a sample made of big monodisperse particles, Fig. 2. Both SANS and SAXS experiments reveal the key role of the small particles for the deswelling process of the big particles. We explain this considering the osmotic pressure in our samples, which is mainly caused by counterions that are free to leave the microgel particles[3]. We show that small particles exert higher osmotic pressure than big particles at the same ζ. We need enough small particles to have an osmotic pressure able to deswell the big particles, allowing the crystallization.

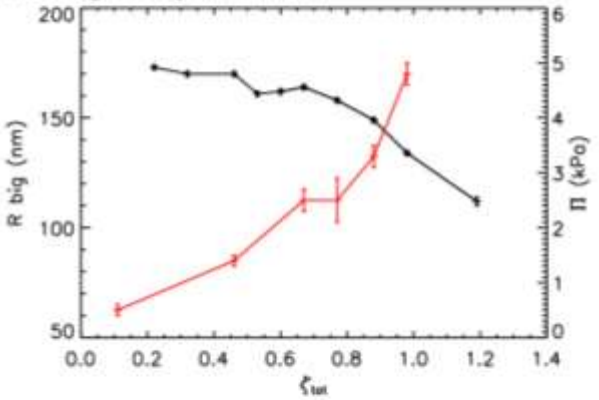

Fig. 1 Variation of the radius of the big particles with ζ is shown. The osmotic pressure is in red.

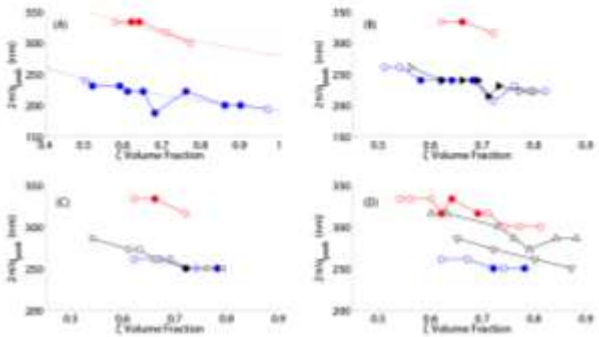

Fig. 2 nnd at different ζ for: monodisperse small particles, monodisperse big particels and binary samples (black symbols) with n_{big} = 0.023 (B), 0.286 (C), and 0.38 and 0.8 (D). Closed symbols represent samples with crystals.

DISCUSSION & CONCLUSIONS: Our results explain the deswelling mechanism in binary suspensions of soft and deformable microgels and justify the observed phase behavior.

REFERENCES: [1] A. St. John Iyer et al.; **2009**; *Angew. Chem.*; 48: 4562-4566

[2] M. Stieger et al.; **2004**; *J. Chem. Phys.*; 120: 6197-6206

[3] R. Borrega et. al; **1999**; *Europhys. Lett.*; 47: 729-735

Swiss Soft Days XV

ENCAPSULATION OF TEMPERATURE SENSITIVE MATERIALS BY ENVIRONMENTALLY CONTROLLED EMULSION ELECTROSPINNING

A. Camerlo[1,2], A.-M. Bühlmann-Popa[1], C. Nardin[2], R.M. Rossi[1], G. Fortunato[1]

[1] *Empa, St Gallen, Switzerland.* [2] *University of Geneva, Switzerland.* giuseppino.fortunato@empa.ch

INTRODUCTION: Emulsion electrospinning is a promising encapsulation method for sensitive materials such as fragrances. However, environmental conditions while electrospinning are of influence not only on the fiber morphology, but also on the encapsulation efficiency (EE) of the fragrance within the nanofibers. An emulsion of limonene dispersed in a PVA aqueous continuous phase was electrospun in various temperature (T) and relative humidity (RH). Thereby, the influence of environment on the fiber structure and encapsulation efficiency of the fragrance was demonstrated. This study is of importance when considering the use of emulsion electrospinning for encapsulation purposes [1].

METHODS: PVA (205000 $g.mol^{-1}$), (R)-(+)-limonene were purchased from Sigma Aldrich (Steinheim, Germany). PVA stock solutions (6 % and 9 %, w/w) were prepared by dissolving the appropriate amounts of PVA in water. Limonene was then dispersed in the PVA continuous phase until reaching respectively a limonene phase/aqueous phase ratio of 1/8 (w/w) Emulsion viscosities were assessed using a Physica MCR301 Rheometer (Anton Paar, Graz, Austria) with a plate – cone geometry linked to a temperature control unit (Anton Paar, Viscotherm VT2, Graz, Austria) containing a 50/50 (w/w) mixture of ethylene glycol and water. The electrospinning took place in a climatic cabin set to 8, 16 and 24 °C and 55, 65, 75, 85 % RH. The fibrous mats obtained were analyzed using scanning electron microscopy (SEM, S-4800, Hitachi, Canada), the encapsulation efficiency was evaluated via Gas Chromatography (GC Trace 2000, Italy) using anisol as internal standard.

RESULTS AND DISCUSSION: The viscosity of the studied emulsions proved to be dependent on PVA concentration in the continuous phase as well as on the temperature. Previous results [2] showed that the fiber morphology was dependent on the PVA concentration in the continuous phase. The change in viscosity due to T was of low influence on the fiber morphology (effect mostly visible on fibers from 9 % PVA concentration in the continuous phase, *Fig. 1*). However, RH influenced the fiber morphology to the highest extent, especially for high values (75 and 85 %). Indeed, in such conditions, the speed of solvent evaporation was decreased, causing the formation of multiple electrical paths leading to jet instabilities and hydrated fibers to reach the collector (*Fig. 1*). The fiber morphology was then compared to the one obtained from a formulation having the same amount of polymer in the continuous phase, but n-hexadecane as a dispersed phase. Fibers formed from these two emulsions showed similar morphologies.

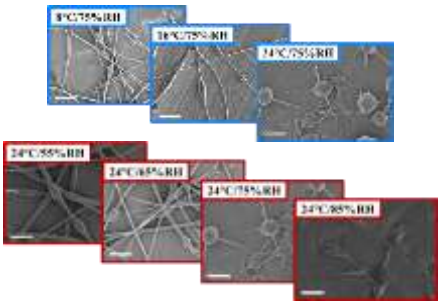

Fig. 1: SEM micrographs of electrospun fibers from a 9 % PVA/limonene emulsion

For the 9 % PVA/limonene emulsion electrospun fibers, both T and RH influenced the fiber EE (*Fig. 2*). At high RH, the fibers remained hydrated, the PVA permeability increased, thus increasing limonene evaporation, in particular at high T.

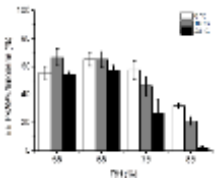

Fig. 2: Limonene EE according to RH and T while electrospinning a 9 % PVA/limonene emulsion

CONCLUSIONS: The fibers produced from a fragrant emulsion are bicomponent of various morphologies and EE according to environmental electrospinning conditions.

REFERENCES: [1] A. Camerlo, **2014**, *J. Mat. Sci.*, DOI 10.1007/s10853-014-8524-5
[2] A. Camerlo, **2013**, *Eur. Polym. J.*, 49, 12:3806-3813.

Optically responsive supramolecular glasses

D. W. R. Balkenende, Christophe A. Monnier, G. L. Fiore & C. Weder

Adolphe Merkle Institute, University of Fribourg, CH-1700, Fribourg, Switzerland.

INTRODUCTION: Optically healable polymers are of great interest because the stimulus can be applied locally [1]. Most healable polymers exhibit relatively weak mechanical properties and exclude a large range of opportunities for applications such as high performance coatings [2]. We introduce supramolecular polymer glasses based on low-molecular weight monomers as a new class of healable materials. The monomer consists of three ureidopyrimidone (UPy) units linked together with a short ethyl spacer. The UPy-based monomer can via hydrogen bonding assemble to form a supramolecular network which behaves like a glassy polymer (Fig 1).

METHODS: The optically responsive supramolecular material was easily synthesized by reacting 1,1,1-tris(hydroxymethyl)propane with three equivalents of 2-(6-isocyanatohexylaminocarbonylamino)-6-methyl-4[1H]pyrimidinone to yield trifunctional $(UPyU)_3TMP$ in 89% yield.

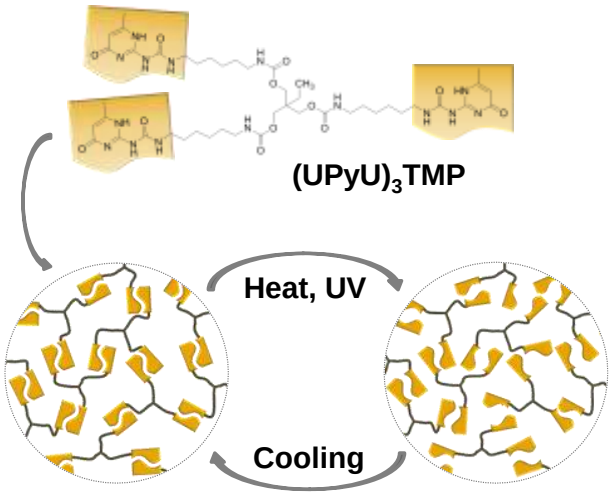

Fig. 1: Schematic representation of the formation of disordered supramolecular networks based on $(UPyU)_3TMP$ and their reversible, heat- or light-induced dissociation.

RESULTS & DISCUSSION: By thermal analysis a glass transition temperature (T_g) of around 50 ºC was observed, and X-ray powder diffraction experiments showed only diffuse scattering, characteristic for amorphous materials. Nanoindentation measurements show a high stiffness at room temperature (3.0 GPa) and the material offers excellent coating and adhesive properties. Instead of transitioning into a low-viscosity liquid, as it is observed for *molecular glasses* above T_g, rheological studies of the UPy-based *supramolecular glass* showed that upon heating above T_g the material shows frequency-dependent storage and loss moduli, indicating polymer like properties. Furthermore, upon irradiation with ultraviolet light, rapid optical healing of damaged surfaces was observed (Fig 2).

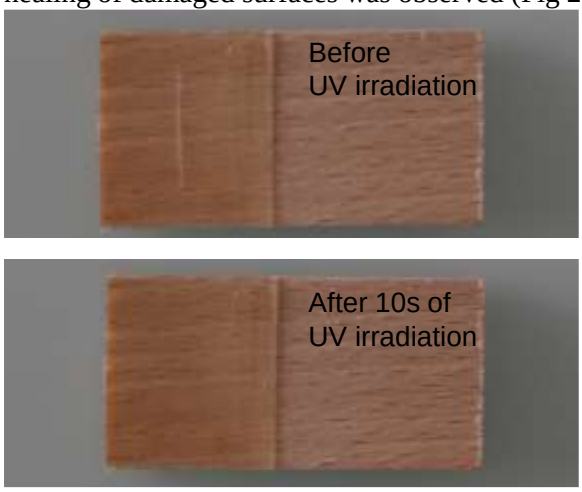

Fig. 2: Images showing the optical healing of a damaged coating on wood. The original 300 µm thin coating was cut with a razor blade (top) and subsequently exposed to the light of a UV lamp for 10 s, which caused complete healing (bottom).

CONCLUSIONS: Our work demonstrates that supramolecular glasses are a promising new class of stimuli responsive materials. This approach can be extended to a broad range of new materials based on supramolecular monomers with other core groups and binding motifs to tune the materials properties.

REFERENCES: [1] C. Weder *et al.*; **2011**; *Nature;* 472: 334-337; [2] C. Weder *et al.*; **2013**; *Chem. Soc. Rev.;* 42: 7278-7288

ACKNOWLEDGEMENTS: This work has been supported by the U.S. Army Research Office (W911NF-12-1-0339), and the Adolphe Merkle Foundation.

Swiss Soft Days XV

Disordered actomyosin contracts in unexpected ways

M. Lenz

LPTMS - CNRS and Université Paris-Sud, Paris, France.

The motion of living cells is in large part due to the interaction of semi-flexible actin filaments (F-actin) and myosin molecular motors, which induce the relative sliding of F-actin. It is often assumed that this simple sliding is sufficient to account for all actomyosin-based motion. While this is correct in our highly organized striated muscle, we question the application of this dogma to less ordered actomyosin systems, thus reexamining a cornerstone of our understanding of cellular motion.

High frequency microrheology of enantiomeric peptide hydrogel networks

P.J. Beltramo[1,2], K.J. Nagy[1,3], J.P. Schneider[3], E.M. Furst[1]

[1] *University of Delaware, Newark, DE, USA.* [2] *ETH Zürich, Zürich, Switzerland.*
[3] *NIH, National Cancer Institute, Frederick, Maryland, USA.*

INTRODUCTION: Self-assembled peptide hydrogels are of particular interest for drug delivery and tissue engineering applications where, for example, biocompatible hydrogels could be used as an artificial cellular scaffold for tissue regeneration in wounds. Applications such as these require control over both the rate of gel formation and the final gel stiffness. Diffusing wave spectroscopy (DWS) offers a noninvasive method to access the high frequency linear rheology of such materials, beyond the capabilities of conventional mechanical rheometers and particle tracking microrheology methods, enabling precise characterization of their mechanical properties.

METHODS: The focus of the current work is the application of DWS techniques to a self-assembling peptide hydrogel known as MAX1. The peptide consists of a 20 amino acid sequence which reversibly folds into a β-hairpin structure upon screening the electrostatic repulsion. Peptide hydrogel networks of 0.75 and 1 wt% MAX1, its enantiomer DMAX1, and their racemic mixture with 1 μm diameter tracer particles are studied. Previous work identified that gels formed from enantiomeric mixtures possess a storage modulus four times as large as those containing either enantiomer [l].

Simultaneous photon counting and multispeckle DWS techniques are used to measure the viscoelastic properties of the gels [2]. The measured mean squared displacement (MSD) of the particles are related to the bulk rheological properties of the medium through the Generalized Stokes-Einstein Relation (GSER) and interpreted using Mackintosh theory [3].

RESULTS: In Figure 1 we plot the MSD nondimentionalized by ρ, the polymer length per unit volume to eliminate the weight percent dependence in the high frequency regime. There are several interesting features of the complete data set. As expected from previous oscillatory rheometry, there is minimal difference between gels formed by MAX1 and DMAX1. The increase in the modulus of the racemic mixture is evident by the decreased magnitude of the long lag time plateau in the MSD. The enhancement increases with increasing peptide concentration. The high frequency (short lag time) MSD scales with $\tau^{3/4}$, as expected for semiflexible polymer networks. From this exponential behaviour the persistence length and bending modulus of the filaments forming the gel network are directly determined.

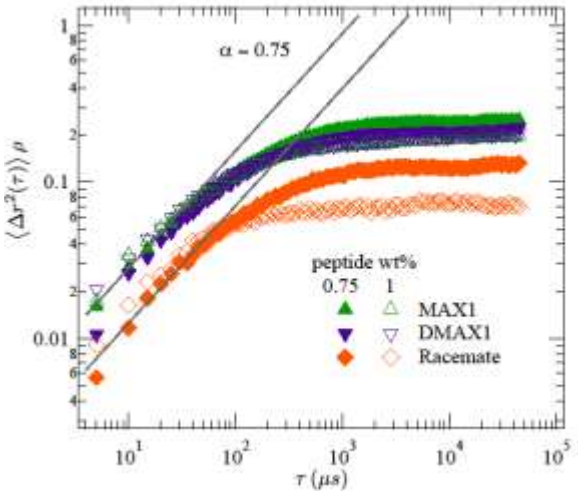

Fig. 1: DWS microrheology of peptide hydrogels.

DISCUSSION & CONCLUSIONS: DWS microrheology effectively measures the peptide mechanical properties. The asymptotic logarithmic scaling of the MSD across all samples indicates the formation of a semiflexible polymer network. The increase in persistence length upon forming the gel from a racemic mixture suggests the enantiomers interact on a molecular level, mixing to form stiffer filaments. As DWS is a passive, non-destructive, measurement technique the results demonstrate its expanded use to characterize hydrogel materials.

REFERENCES:

[1] K.J. Nagy *et al*; **2011**; *JACS*; 133:14975-14977.

[2] F. Scheffold and P. Schurtenberger; **2003**; *Soft Materials*; 1:139-165.

[3] F.C. MacKintosh *et al*; **1995**; *PRL*; 75:4425-4428.

Swiss Soft Days XV

Polymer dynamics in self-assembled block copolymer membranes

F. Itel[1], M. Chami[2], A. Najer[1], D.Wu[1], S. Lörcher[1], I. A. Dinu[1], W. Meier[1]

[1]Department of Physical Chemistry, University of Basel, Switzerland. [2]C-CINA, Biozentrum, University of Basel, Switzerland

INTRODUCTION: Membranes provide barriers to protect and store active entities in a confined space for proper function. Amphiphilic block copolymers self-assemble into artificial membranes of enhanced strength and stability compared to lipid membranes.[1] In addition, these membranes are still able to incorporate biological membrane proteins.[2] Membrane fluidity is a key parameter for retaining function of incorporated proteins. The lateral mobility and deduced membrane organizations reveal insight into structural aspects at the molecular level. From a structural point of view, amphiphilic block copolymers within a self-assembled membrane adopt much more complex structures. In this respect, we studied important membrane properties, such as lateral diffusion coefficients, domain formation, membrane thickness and membrane viscosity of artificial membranes based on diblock (A_xB_y) and triblock ($A_xB_yA_x$) copolymers containing poly(2-methyl-2-oxazoline) (PMOXA – hydrophilic A-block) and poly(dimethylsiloxane) (PDMS – hydrophobic B-block) known to form polymersomes and incorporate membrane proteins in aqueous solution.[3,4,5]

METHODS: In order to determine lateral diffusion coefficients and to investigate the membrane structure, a large library of diblock and triblock copolymers with different molecular weights was synthesized. Z-scan fluorescence correlation spectroscopy (FCS) was used to determine lateral diffusion coefficients on membranes of giant unilamellar vesicles (GUVs) and to retrieve information about the existence of rafts and domain structures below the refraction limit of the laser beam.[6] Cryogenic transmission electron microscopy (Cryo-TEM) was performed to determine membrane thicknesses of self-assembled polymersomes in order to deduce the chain conformation of the polymer molecules within the membrane.

RESULTS: The lateral diffusion coefficients (D) scale with the molecular weight of the hydrophobic block (M_h) for both diblock and triblock configurations as $D \sim M_h^{-1.25}$. A significantly increased diffusion of diblocks compared to triblocks reveals that the diffusion is primarily related to the different structural conformation of the macromolecules assembled in the membrane. Moreover, hindered diffusion for higher molecular weight copolymers is observed, indicating formation of domains due to interdigitation and entanglement, whereas free 2D diffusion is detected for low molecular weight copolymers

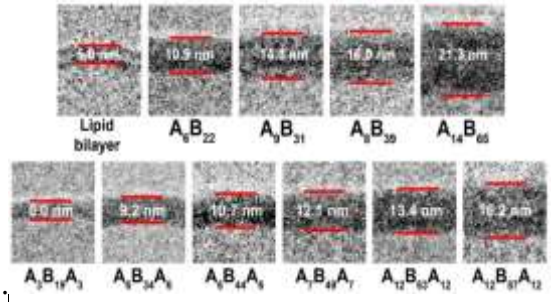

Fig. 1: Systematic view of diblock (upper panel) and triblock (lower panel) copolymer membranes arranged with increasing membrane thickness (from left to right). A-block: PMOXA; B-block: PDMS. Images were generated by cryo-TEM technique.

DISCUSSION & CONCLUSIONS: The results represent a further step to understand structure-related membrane properties, i.e. density, stability, fluidity, permeability, etc.[7] Additionally, the tracking of labeled membrane constituents embedded in artificial membranes offers crucial information about the desired functionality of bio-inspired supramolecular 3D nano-assemblies.

REFERENCES:

[1] Discher, B. M.; Won, Y. Y.; Ege, D. S.; Lee, J. C. M.; Bates, F. S.; Discher, D. E.; Hammer, D. A. *Science* **1999**, *284*, 1143-1146.

[2]Nardin, C.; Thoeni, S.; Widmer, J.; Winterhalter, M.; Meier, W. *Chem. Comm.* **2000**, 1433-1434.

[3]Bates, F. S.; Fredrickson, G. H. A*nn. Rev. Phys. Chem.* **1990**, *41*, 525-557.

[4]Tanner, P.; Baumann, P.; Enea, R.; Onaca, O.; Palivan, C.; Meier, W. *Acc. Chem. Res.* **2011**, *44*, 1039-1049.

[5]Wu, D.; Spulber M.; Itel F.; Chami M.; Palivan C.G.; Meier W. *Macromolecules* **2014**, 47, 5060-5069.

[6]Benda, A.; Benes, M.; Marecek, V.; Lhotsky, A.; Hermens, W. T.; Hof, M. *Langmuir* **2003**, *19*, 4120-4126.

[7]Itel, F., Chami M., Najer A., Lörcher S., Wu D., Dinu I.A., Meier W., *submitted.*

Swiss Soft Days XV

Structured Device Materials By Polymer Self Assembly

Ullrich Steiner

Adolphe Merkle Institute, Rue des Verdiers, CH-1700 Fribourg

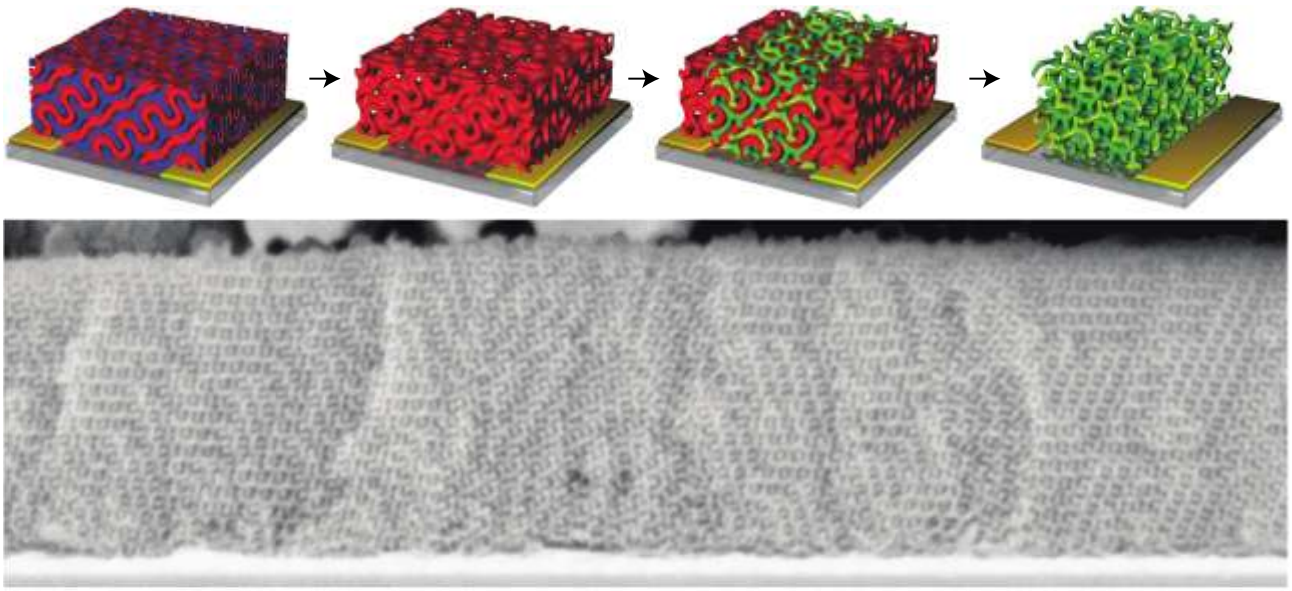

Polymer self assembly is well established for the structure formation in polymer melts on the 10-nm length scale. The translation of organic self-assembly into functional materials is however not straight forward. 10-nm morphologies in these materials are desirable since the function of a wide range of materials does not only depend on their intrinsic (chemical, mechanical, electronic, optical) properties, but also how the material is assembled on length scales from 10 nm to the macroscale. The careful control of material architectures therefore often enables performance enhancements, eliminating the need to develop new material chemistries. My presentation will introduce several approaches how to structure metals metal oxides, and polymers on length scales ranging from 10 nm to several µm. These structural motives are introduced into the materials by polymer self-assembly and the self-organisation of colloids and materials synthesis methods include electrochemical deposition, sol-gel chemistries and chemical vapour processes. The resulting structured materials improve the performance of dye-sensitised solar cells, super-capacitors, optical metamaterials, and optical coatings.

Scanning Tunneling Microscopy Characterization of Gold Nanoparticles: Morphologies of The Ligand Shell

Quy Ong, Francesco Stellacci

Institute of Materials Engineering, EPF Lausanne, Lausanne, Switzerland..

Gold nanoparticles are composed of a core protected by a ligand shell of a self-assembled monolayer (SAM). This SAM determines largely a number of surface and interfacial properties. The design of the ligand shell is made possible with thiolated ligands thanks to the strong sulphur-gold bond. Frequently, the ligand shell is designed to compose of multiple types of molecules to provide the particles with a certain set of properties and sometime novel properties show up that cannot be explained by shell composition. It was discovered that the shell ligand molecules arrange into patches leading to structure-dependent properties. Different types of such patches are found and studied by scanning tunneling microscopy (STM).

For a certain binary combination of thiolated molecules, it has been discovered that the ligand shell has an unusual morphology in which thiols self-assemble into ripples or stripe-like domains of alternating composition. Along a stripe, the distance between two nearest thiols is ~0.5 nm, and in the perpendicular direction, the stripe spacing is ~1nm. Examples of such structure are given in Figure 1 and 2. The distance of ~0.5 nm in the compact direction is also found in ligand shells of homoligand coated nanoparticles where quasi-hexagonal order exists. Ligand shells of some binary mixtures are found to de-mix completely resulting in the Janus structure as exemplified in Figure 3.

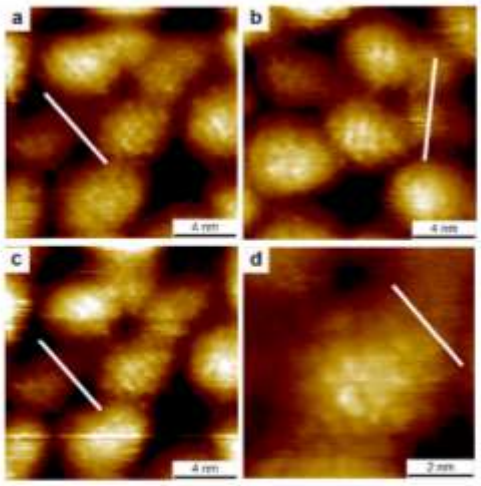

Fig. 1: STM topography images of gold nanoparticles coated with a mixture of nonanethiol and methylbenzenethiol recorded at different scan angles and scan lengths. White strips on the images are added to show the orientations of stripe-like domains.

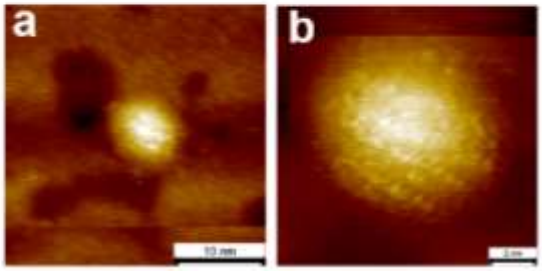

Fig. 2: STM topography images of a gold nanoparticle coated with a mixture of mercapto-propionic acid and octanethiol at two different scanning lengths. Stripe-like domains are resolved to show the linear order of thiolated ligands.

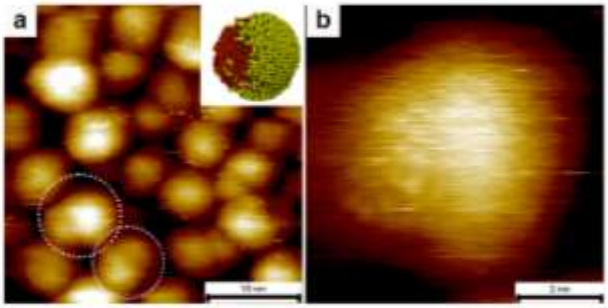

Fig. 3: STM topography images of a gold nanoparticle sample coated with 11-Mercapto-1-undecanol (C11ol) and 4-Mercapto-1-butanol (C4ol), showing multiple nanoparticles possess the Janus structure in (a). Examples are given by white circle markings. Higher resolution of a Janus particle is given in (b).

1. Q. K. Ong, S. Zhao, J. Reguera, F. Biscarini and F. Stellacci, *Chem. Comm.*, **2014**, 50, 10456.
2. Q. K. Ong, J. Reguera, P. J. Silva, M. Moglianetti, K. Harkness, M. Longobardi, K. S. Mali, C. Renner, S. De Feyter and F. Stellacci, *ACS Nano*, **2013**, 7, 8529.
3. M. Moglianetti, Q. K. Ong, J. Reguera, K. Harkness, M. Mameli, A. Radulescu, J. Kohlbrecher, C. Jud, D. Svergun and F. Stellacci, *Chem. Sci.*, **2014**, 5, 1232.
4. F. Biscarini, Q. K. Ong, C. Albonetti, F. Liscio, M. Longobardi, K. S. Mali, A. Ciesielski, J. Reguera, C. Renner, S. De Feyter, P. Samori and F. Stellacci, *Langmuir*, **2013**, 29, 13723.
5. A. M. Jackson, J. W. Myerson and F. Stellacci, *Nat. Mater.*, **2004**, 3, 330-336.

Abstracts for the posters

Effect of the Interaction of the Amyloid β (1-42) Peptide with Short Single Stranded Synthetic Nucleotide Sequences

*Jancy Nixon Abraham, Dawid Kedracki, Enora Prado, Charlotte Gourmel, Plinio Maroni and Corinne Nardin**

University of Geneva, Faculty of Sciences, Department of Inorganic and Analytical Chemistry, Quai Ernest Ansermet 30, CH-1211, Geneva 4, Switzerland

INTRODUCTION: Alzheimer's disease (AD) is a fatal, progressive illness characterized by memory loss, cognitive deficits and behavioral changes. Structural and kinetics features evidence that the disease is associated to a protein folding disorder: the amyloid Aβ (1-42) proteins (Aβ42) indeed organize into senile or diffuse plaques and vascular deposits according to a nucleation dependent polymerization process. Since amyloidosis is accompanying several diseases, the mechanism of peptide fibril formation is thus currently widely studied. Since the oligomers and fibers are currently assigned as toxic, the present approach is focused on identifying how to both inhibit fibril formation and disassemble fibrils. Although coupling of nucleotide and peptide sequences to synthetic polymers to induce their self-assembly in aqueous solution has been investigated recently, the formation of (micellar) interpolyelectrolyte complexes (IPECs) between a nucleotide and a peptide sequence is scarcely reported.

METHODS: Aβ fibrils were prepared by diluting 5 mM Aβ 42 peptides in DMSO to 100 µM with 10 mM HCl (pH=2), followed by 30 seconds vortexing and incubation at 37 °C for 24 h. The solution was further diluted with water to 10 µM and imaged by AFM. Incubation with either synthetic polymers or nucleic acid strands was performed by adding 500 µM nucleotide sequences and incubation was carried out under the same conditions as for growing fibers. Incubation of nucleic acid strands with fibers was performed by adding a 10 µM solution of amyloid fibers to a 50 µM solution of oligonucleotides and incubating at room temperature for 1 hour. The solution was directly used for AFM measurements.

RESULTS: The fibril formation was inhibited upon incubation of the peptide with nucleotide sequences. Ill-defined structures were observed instead, when the $A\beta_{42}$ peptide was incubated with 5'-AAAGAGAGAGAG-3' (12-mer), 5'-CTAGTCGACTAG-3' and 5'-TCTGAG-3'. Again, subsequent to incubation of Aβ fibrils with the nucleotide sequences, fibrils are no longer visible whereas small spherical structures are observed.

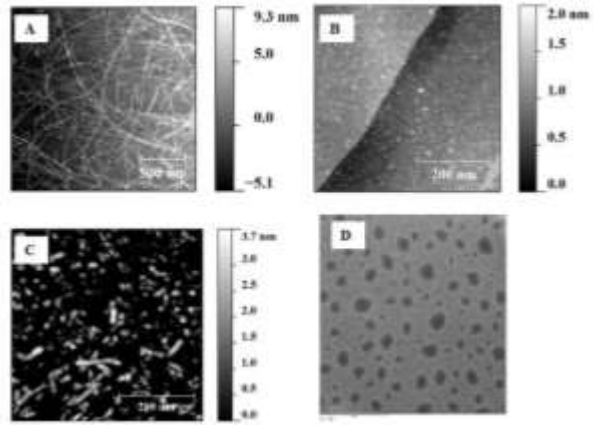

Fig. 1: AFM images of Aβ 42 fibers (A), fiber growth inhibition (B), fiber disassembly(C) and TEM images of IPECs (D).

DISCUSSION & CONCLUSIONS: In this work, we have demonstrated the inhibition of amyloid fibril genesis as well as disassembly of fibers on incubation with oligonucleotides. Irrespective of the length and composition of the nucleotide sequences, the incubation with $A\beta_{42}$ resulted in inhibition of fibril growth. Instead, small spherical structures with an average size of 150 nm were formed. IPECs are probably formed between the peptide and either synthetic polyions or nucleic acid strands, through interaction between monomers or nucleic acids and amino acids of opposite charges. Incubation of the amyloid fibers with synthetic oligonucleotide sequences induces their disassembly.

ACKNOWLEDGEMENTS: The University of Geneva and the SNSF (PPOOP2-128380) are greatly acknowledged for financial support.

REFERENCES:

Abraham. J. N., Kedracki,D., Prado,E., Charlotte Gourmel,C., Maroni, P and Nardin, C. Biomacromolecules 2014, 15, 3253−3258.

Contact Angle at the Leading Edge Controls Cell Protrusion Rate

C. Gabella[1], E. Bertseva[1.2], C. Bottier[1], N. Piacentini[1], A. Bornert[1], S. Jeney[2], L. Forró[2], I. F. Sbalzarini[3], J.-J. Meister[1], A. B. Verkhovsky[1]

[1] Laboratory of Cell Biophysics, EPF Lausanne, Switzerland, [2] Laboratory of Physics of Complex Matter, EPF-Lausanne, Switzerland, [3] MOSAIC Group, Max Planck Institute of Molecular Cell Biology and Genetics, Dresden, Germany.

INTRODUCTION: Plasma membrane tension and the pressure generated by actin polymerization are two antagonistic forces believed to define the protrusion rate at the leading edge of migrating cells [1, 2]. Quantitatively, resistance to actin protrusion is a product of membrane tension and mean local curvature (Laplace's law); thus, it depends on the local geometry of the membrane interface. However, the role of the geometry of the leading edge in protrusion control has not been yet investigated. Here, we manipulate both the cell shape and substrate topography in the model system of persistently migrating fish epidermal keratocytes. We find that the protrusion rate does not correlate with membrane tension, but, instead, strongly correlates with cell roundness, and that the leading edge of the cell exhibits pinning on substrate ridges – a phenomenon characteristic of spreading of liquid drops. These results indicate that the leading edge could be considered a triple interface between the substrate, membrane and the extracellular medium, and that the contact angle between the membrane and the substrate determines the load on actin polymerization and, therefore, the protrusion rate (Figure A, B). Our findings thus illuminate a novel relationship between the three-dimensional shape of the cell and its dynamics, which may have implications for cell migration in three-dimensional environments **[3].**

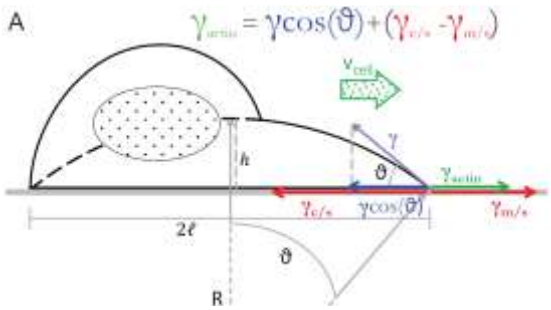

Fig. A: Diagram of the force balance for the triple interface at the leading edge showing the contributing forces and dimensions used for determining membrane curvature and contact angle. Lamellipodium height is exaggerated for clarity. Thick green arrow indicates the direction of cell motion. On top, the equation of the force balance is shown.

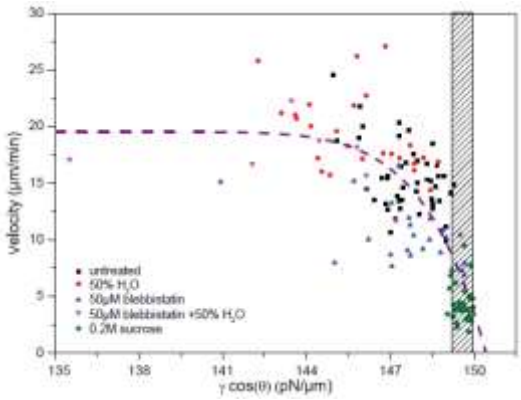

Fig. B: Plot of protrusion velocity versus membrane load estimated from the contact angle at the leading edge for cells under different conditions. The dark band represents the interval of load values estimated for the lateral extremities of the cells, where protrusion stalls. To help visualizing the trend, data are fitted (dashed line) according to [4], in the form of $v = v_0(1 - (\gamma\cos\theta - 90)/F_s)^w)$, *with* $w = 7.10$, $F_s = 10.28\ pN/\mu m$ *and* $v_0 = 19.54\ \mu m/min$.

REFERENCES:

[1] Mogilner, A., and Zhu, J. (2012). Curr Biol 22, R48-R51.

[2] Raucher, D., and Sheetz, M.P. (2000). J Cell Biol 148, 127-136.

[3] Gabella, C. et al. (2014). Curr Biol 24, 1126-1132

[4] Keren, K., et al. (2008). Nature 453, 475-480

Swiss Soft Days XV

"Active Surfaces" Formed by Immobilization of Enzymes on Solid-Supported Polymer Membranes

Justyna Kowal[1], Camelia Draghici[1,2], Alina Darjan[2], Wolfgang Meier[1], Cornelia G. Palivan[1]

[1] *University of Basel, Klingelbergstrasse 80, 4056 Basel, Switzerland*
[2] *Transilvania University of Brasov, 29 Eroilor Blv, 500036 Brasov, Romania*

INTRODUCTION: Solid-supported membranes serve as novel systems to generate active surfaces, with possible applications in various domains, such as medicine, or enviornmantal sciences.[1] Here we present the design of planar membranes, based on solid-supported bilayers of asymmetric amphiphilic triblock copolymers to serve as templates for combination with enzymes and development of "active surfaces".[2]

METHODS: A group of poly(ethylene glycol)-*block*-poly(γ-methyl-ε-caprolactone)-*block*-poly[(2-dimethylamino) ethyl methacrylate] copolymers, with different hydrophilic and hydrophobic domains (PEG_{45}-$PMCL_X$-$PDMAEMA_Y$) was selected to generate solid-supported polymer membranes. The molecular arrangements of the copolymers at the air-water interface were established by a combination of Langmuir isotherms and Brewster angle microscopy. Polymer films were transferred by Langmuir-Blodgett technique to solid-substrate for further characterization and functionalization with laccase.

RESULTS: Uniform thin layers of copolymers were obtained by transferring films onto silica solid supports at optimal surface pressure. These solid-supported polymer membranes were further characterized by assessing properties such as monolayer film thickness, hydrophilic/hydrophobic balance, topography and roughness. Activity assays showed that immobilized enzyme preserved its activity.

DISCUSSION & CONCLUSIONS: Laccase, used as enzyme model, was successfully attached to copolymer membranes by stable interactions. The interaction between the amphiphilic triblock copolymer films and immobilized enzymes represents a straightforward approach to engineer "active surfaces", with biomolecules playing the active role by their intrinsic bioactivity.

REFERENCES:

(1) Kowal, J.; Zhang, X.; Dinu, I. A.; Palivan, C. G.; Meier, W. *ACS Macro Letters* 2014, *3*, 59.

(2) Draghici, C. L.; Kowal, J.; Darjan, A.; Meier, W.; Palivan, C. G. *Langmuir* 2014 (accepted).

Swiss Soft Days XV

A single polymer chain as a nanocarrier for multiple proteins delivery with regulated pH responsiveness

J.Liu, V.Postupalenko, D.Wu, M.Spulber, C.G. Palivan, W.Meier

University of Basel, Basel, Switzerland.

INTRODUCTION: Polymer conjugates and polymeric carriers play an important role for the development of protein therapy. Proteins shielded by these polymeric systems can avoid the fast recognition by the immune system and the digestion by proteolysis, prolonging their circulation time in blood. However, a consequence of polymer conjugation is generally a loss of protein biological activity. The loading capacity of proteins in polymeric carriers is hard to improve and their elimination from the body can be problematic.

In this work, we present a novel concept using single polymer chain as nanocarriers for the delivery of multiple proteins with regulated pH responsiveness. The polymers bearing multiple tris-nitrilotriacetic acids (trisNTA) are complexed with metal cations and serves for the binding of His-tagged proteins.[1] His-tagged enhanced yellow fluorescent protein (eYFP) is chosen as the model for the study. We try to control two factors: coordination center and distance between trisNTA binding sites, in order to regulate the stability of the conjugation and the pH responsiveness. The low molecular weight of polymers allows their full eliminations from the body after pH-triggered release of loaded proteins.

METHODS: The binding affinity of Me^{2+}-loaded trisNTA-functionalized polymers (Me^{2+}-PNTs) with different average distance between binding sites and eYFP was determined by isothermal titration calorimetry (ITC). The stability and the pH responsiveness of polymer-protein conjugates was analyzed by fast protein liquid chromatography (FPLC). The stability of proteins before and after release from the polymers was investigated by circular dichroism (CD) and fluorescence spectroscopies. The cell viability was assessed by MTS assay.

RESULTS: ITC results showed that the dissociation constant of PNT-Me^{2+}-eYFP conjugates varied from 1.35±0.12 µM to 0.07±0.01 µM depending on the loaded-cations in trisNTA pockets and the average distance between trisNTA binding sites. PNT1 and PNT4, which maximal average distance between trisNTA binding sites is 31.5 nm and 5.2 nm, respectively, were employed for the following studies. PNT4-Cu^{2+}-eYFP showed the highest stability but had no significant pH-triggered release of eYFP until the pH was dropped to 5. PNT4-Zn^{2+}-eYFP exhibited a significant pH-triggered release of eYFP at both pH 6 and 5 (Fig. 1). The decrease of average distance between trisNTA binding sites significantly enhanced the stability of the conjugates, for the case of PNT4-Zn^{2+}-eYFP and PNT1-Zn^{2+}-eYFP, which was attributed to the interactions between proteins and steric hindrance.

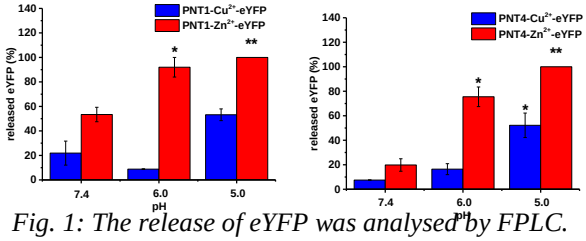

*Fig. 1: The release of eYFP was analysed by FPLC. Stars indicate significance in two-tailed Student's t-test; *P<0.05, **P<0.005.*

No influences of the structure and the function of eYFP were observed by CD and fluorescence spectroscopies before and after release from the PNTs. Moreover, PNTs-Zn^{2+} didn't exhibit any cell toxicity assessed by MTS assay.

DISCUSSION & CONCLUSIONS: The stability and pH responsiveness of PNTs-Me^{2+}-eYFP were successfully regulated by the adjustment of coordination metals in the trisNTA pockets and by controlling the average distance between trisNTA binding sites. The decrease of average distance between trisNTA binding sites significantly enhanced the stability of the conjugates, which was attributed to the interactions between proteins. In addition, the pH responsiveness of PNTs-Me^{2+}-eYFP wasn't influenced by the adjustment of average distance between trisNTA.

REFERENCES: [1] J. Liu; **2014**; *J. Am. Chem. Soc.;* 136:12607-12614.

ACKNOWLEDGEMENTS: We thank the Swiss National Science Foundation, and the University of Basel for financial support. J. L. thanks China Scholarship Council for supporting the fee to study abroad.

Swiss Soft Days XV

Multifunctional Microcapsules With Macroporous Polymer Shells

E.Loiseau[1], M.Frey[1], Y.Blickenstorfer[1], A.Hauser[1], F.Niedermair[2], A. Studart[1]
[1] *Complex Materials, ETH Zurich, Zurich , Switzerland.*
[2] *BASF Construction Solutions GmbH, Trostberg, Germany*

Microcapsules are of great interest in biomedical applications, the food industry, cosmetics and as catalyst supports. Multifunctional capsules that respond to more than one stimuli are needed in many of these applications to achieve controlled release and enable smart manipulation. A wide variety of release patterns, including passive or active, one-time or multiple, sequential or simultaneous have been achieved by tailoring the chemistry and structure of the microcapsules [1].

Here, we demonstrate a novel method to obtain microcapsules with polymer shells of controlled macroporosity and mechanical properties that can be tuned within a wide range. These capsules contain two liquid compartments: an aqueous core and an oil phase that permeates the macroporous polymer shell. Simultaneously loading of water-soluble chemicals in the core and oil-soluble chemicals in the liquid phase of the biphasic shell can potentially enable the creation of capsules that respond to multiple external stimuli.

Microcapsules are produced by microfluidics, using a co-flow flow-focusing glass capillary device to make water-oil-water (W/O/W) double emulsion templates. A mixture of acrylate monomers (glycidyl methacrylate and ethylene glycol dimethacrylate) and porogens (phthalate-based, alkane or alkanol) is used as oil phase. Heterogeneous polymerization of the acrylate monomers leads to a biphasic structure: a network of polymer particles permeated by the liquid porogen and covered with a thin, tight polymer skin [2]. The diameter of the polymer particles and the pore size can be tuned by varying the amount of porogen or by mixing porogens with different solubility parameters (fig. 1).

The permeability of the shell is determined either by the polymer skin or by the porous structure. Thick polymer skins and close-cell porous shells obtained with low porogen amounts lead to tight capsules, whereas shells with porous skins and open interconnected pores exhibit controlled permeability.

Compression tests of single capsules show that the elastic modulus and the force at break depend on the microstructure of the porous network. Highly interconnected networks of many small polymer particles lead to strong and stiff capsules, while larger and fewer particles result in weaker microcapsules.

The interstitial liquid porogen can also be loaded with an oil-soluble encapsulant or used as carrier for a chemical trigger. In a proof of concept, alkanol with low boiling (pentane, cyclopentane, cyclohexane) point were used as porogen and the resulting temperature-sensitive capsules open when submitted to a thermal shock.

Incorporation of glycidyl methacrylate monomers results in polymer particles with epoxy-functionalized surfaces, which can be further reacted with amine-based functional compounds [3]. We exploited such surface amine groups to create magnetic capsules by covalently binding nitrodopamine-coated iron oxide nano-particles to the outer shell surface.

The proposed multi-compartment structure with functionalizable surface provides a rich platform for the future design of microcapsule systems capable of responding to multiple external stimuli.

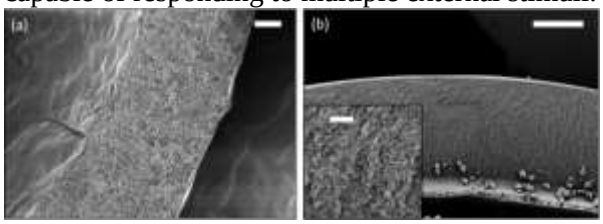

Fig. 1 SEM images from the cross-section of a macroporous microcapsules with 35 wt% di-isodecyl phthalate (a) and 35 wt % diethyl phthalate (b). Scale bar : 5 µm ; inset : 500 nm.

REFERENCES: [1] J.S. Sander, A.R. Studart; **2013**; *Langmuir*; 29(49):15168-15173. [2] S. Dubinsky, et al.; **2008**; *Macromolecules*; 41(10):3555-3561. [3] T. Kaufmann et al.; **2011**; *Advanced Materials*; 23(1): p. 79-83.

ACKNOWLEDGEMENTS: We thank Dr. Jonathan Sander. Tobias Niebel and Dr. Elena Tervoort-Gorokhova for the fruitful discussion. We thank BASF Construction Solution GmbH for financial support.

Swiss Soft Days XV

Polymer membranes with preserved architecture sensitive for protons, monovalent, and divalent cations

M. Lomora[1], M. Spulber[1], F. Itel[1], C. Palivan[1]

[1] *University of Basel, Basel, Switzerland.*

INTRODUCTION: Ion exchange is vital for the cell integrity and functionality, as for example electrical signalling within biological organisms which are in general driven by ions. The lipids phase of the biological cell membranes exhibit a low dielectric constant, and block the passage of small ions, therefore the ion exchange can occur only through various ion channels embedded into the membrane. Using polymer membranes with embedded biopores, but with a preserved architecture, is an elegant approach of mimicking cellular membranes[1].

METHODS: Synthetic polymer vesicles were formed by film rehydration technique and inside their cavity a sensitive fluorescent dye for pH, Na^+, K^+, and Ca^{2+} was used for entrapment inside the vesicles. Dynamic and static light scattering (DLS/SLS), as well as transmission electron microscopy (TEM) was used to test the self-assembly of a triblock copolymer into vesicular structures. The encapsulation of dyes was evaluated by fluorescence correlation spectroscopy (FCS). Insertion of specific biopores into polymer membranes and the ion influx was demonstrated by fluorescence spectroscopy.

RESULTS: Light scattering data indicated formation of nanostructures with a hydrodynamic radius (*Rh*) and a radius of gyration (*Rg*) of ≈ 100 *nm*. These data was further modelled based on form factor ($\rho \approx 0.90$) indicating the presence of vesicular structures. These values were in accordance with the diameter ($d \approx 100\text{-}200$ *nm*) of the observed round-shape structures in TEM. FCS revealed average diffusion times of *16-30* μs for the free dye and a *2500 - 3500* μs for the vesicles containing dyes, from which we concluded that the dyes were encapsulated in the vesicles. By varying the intra or extra-vesicular ion concentrations and adding the biopores into the system, an increase or decrease in the fluorescence intensity of the dyes was observed, concluding that the polymeric membranes were permeabilized towards protons, monovalent and divalent cations.

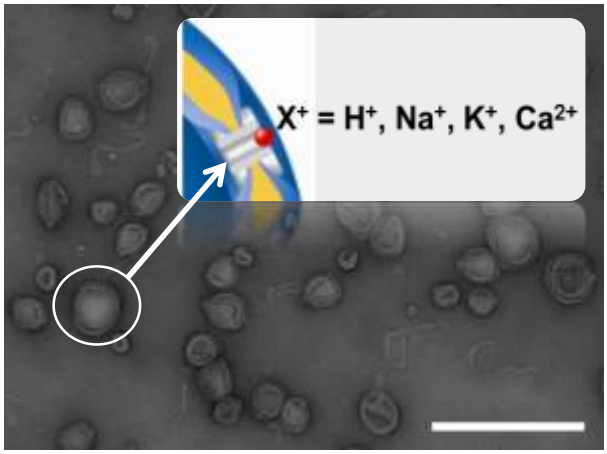

Fig. 1: Conceptual figure for monovalent and divalent sensitive polymer membranes.

DISCUSSION & CONCLUSIONS: We offer here an example of mimicking the cell membrane using a simplistic, but stepwise approach. The successful permeabilization of synthetic polymer membranes with inserted biopores and preserved architecture provides a solution for more complex systems, such as development of nanoreactors, or artificial cells.

REFERENCES:

[1] G. Gunkel-Grabole; 2014; Biomaterials Science; DOI: 10.1039/C4BM00230J.

ACKNOWLEDGEMENTS: We thank G. Persy, University of Basel, for helping us with TEM measurements. We gratefully acknowledged the financial support received by the Swiss Nanoscience Foundation.

Viscoelasticity and Interface Bending Properties of Lecithin Reverse Wormlike Micelles Studied by Diffusive Wave Spectroscopy in Hydrophobic Environment

I.Martiel[1], L.Sagalowicz[2], R.Mezzenga[1]

[1] Food and Soft Materials Science, Institute of Food, Nutrition & Health, ETH Zurich, Zurich, Switzerland. [2] Nestlé Research Center, Vers-Chez-Les-Blanc, CH-1000 Lausanne 26, Switzerland.

Upon the addition of minute quantities of water into a phosphatidylcholine (PC) solution in certain organic solvents, PC micelles elongate into giant reverse wormlike micelles that entangle and form highly viscous microemulsions, called lecithin organogels. We investigated the microrheological properties of concentrated PC-cyclohexane reverse wormlike micellar systems by Diffusive Wave Spectroscopy (DWS) in apolar medium, combined with bulk shear rheology. We adapted water-continuous DWS to our oil-continuous system by using hydrophobic poly(hydroxystearic acid)-grafted PMMA particles as monodisperse tracer particles. Relevant parameters such as the micellar scission energy and persistence length were extracted from the microrheology data and interpreted according to the sphere-to-rod-to-sphere structural transition. Based on these quantities, we calculated the bending and saddle-splay moduli of the PC-covered water-cyclohexane interface (Schematic 1). This approach represents a new method for the quantitative estimation of these fundamental parameters, which are thought to underpin the self-assembly of surfactants.

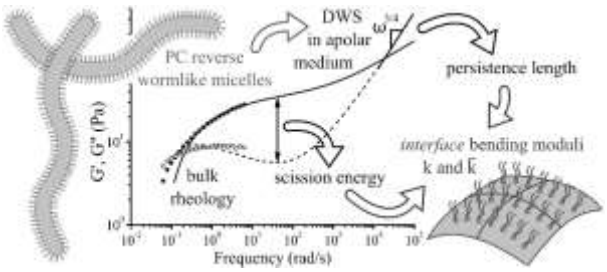

Schematic 1: Micellar scission energy and persistence length give access to the bending properties of the surfactant-covered interface.

REFERENCES:

[1] I. Martiel, L. Sagalowicz, R. Mezzenga; **2014**; *Langmuir;* doi:10/1021/la502748e.

[2] I. Martiel, L. Sagalowicz, R. Mezzenga; **2014**; *Adv. Colloid Interface Sci.;* 209:127-43.

ACKNOWLEDGEMENT: This study was funded by NESTEC Ltd.

3D Woodpile Photonic Crystals with a nearly-complete band gap in the near-infrared

N. Muller[1], C. Marichy[2], F. Scheffold[1]

[1] *Department of Physics and Fribourg Center for Nanomaterials, University of Fribourg, Fribourg, Switzerland.* [2] *University of Lyon, Lyon, France.*

INTRODUCTION: Photonic crystals (PCs) are materials with a periodic modulation of dielectric properties. These materials can exhibit complete photonic band gaps; frequency regions for which the propagation of electromagnetic radiation is forbidden due to depletion of the density of states. It would thus be possible to control the flow of light by engineering optical circuits embedded inside PCs. Therefore direct or inverted woodpiles made of high refractive index material like silicon, germanium or titanium dioxide (TiO_2) are sought after.

METHODS: Three-dimensional woodpile PCs were fabricated by direct laser writing based on multi-photon absorption in a polymer based photosensitive material.[1] The next processing step consists in infiltrating the as-fabricated PCs via atomic layer deposition (ALD) with amorphous titanium dioxide. The high quality of the structures during the different manipulation processes is shown in figure 1. A further temperature treatment at 600°C for several hours allows for the calcination of the polymer and the conversion of the amorphous titania to its denser anatase phase which exhibits a slightly higher index of refraction. Optical measurements were performed with a commercially available Fourier transform infrared spectrometer (Vertex 70 Bruker) connected to a microscope (Hyperion 2000 Bruker).

RESULTS: By tuning the number of ALD cycles we succeeded to pass from a partially infiltrated scenario to a completely infiltrated one, which presents strong photonic features. FTIR optical measurements were taken after the temperature treatment and in the near-infrared we observe the presence of a strong peak in reflectance and a corresponding dip in transmittance (cf. figure 2). Note that the optical features are shifted towards larger wavelengths and broaden during the infiltration process, a hallmark for an increased index of refraction contrast. These spectral features can be attributed to scattering from Bragg planes inside the photonic crystal and are an evidence for the presence of a nearly-complete photonic band gap in the near-infrared.

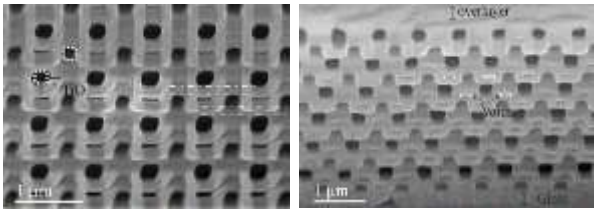

Fig. 1: Scanning electron microscopy images of focused ion beam etched woodpile PCs partially (left) and completely infiltrated (right) with titanium dioxide.

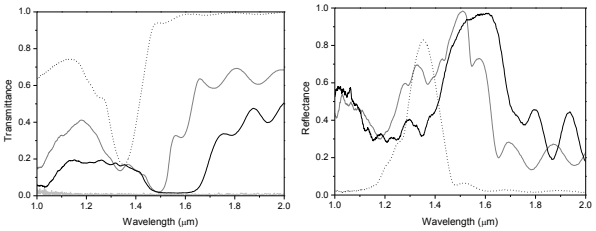

Fig. 2: FTIR transmittance (left) and reflectance (right) measurements of the as-fabricated woodpile photonic crystals taken at different infiltration steps (dotted: polymer, grey: partially infiltrated and black: completely infiltrated).

DISCUSSION & CONCLUSIONS: In the current work, a novel one step-infiltration technique for fabricating three-dimensional woodpile PCs with titania presenting a nearly-complete photonic band gap has been demonstrated.

REFERENCES: [1] M.Deubel, M. Wegener. Appl. Phys. Lett.; **2005**; 87:221104.

ACKNOWLEDGEMENTS: The present project has been financially supported by the National Research fund, Luxembourg (Project No. 3093332), the Swiss National Science Foundation (Project No. 132736 and 149867) and the Adolphe Merkle Foundation.

Influence of the Potential Barrier on the Breakage Rate of Colloidal Aggregates in Simple Shear and Elongational Flows

Zhiqiang Ren[1], Yogesh M. Harshe[2] and Marco Lattuada[1]

[1] *Adolphe Merkle Institute, University of Fribourg, 1700-Fribourg, Switzerland*

[2] *Department of Chemical Engineering, Delft University of Technology, The Netherlands.*

INTRODUCTION: Understanding the effect of interparticle interactions on the breakage rate of colloidal clusters is of crucial importance to better design nanoparticles redispersion and coagulation processes. In this work we build on our previous paper[1] and compute the breakage rate of colloidal aggregates under simple shear and elongational flows by means of Stokesian Dynamics simulations.

METHODS: A library of clusters made of identical spherical particles covering a broad range of masses and fractal dimension values (from 1.8 to 3) was generated by means of a combination of several Monte-Carlo methods. The hydrodynamic interactions among the particles have been accounted for by Stokesian Dynamics. DLVO theory has been used to describe the interparticle interactions, while contact forces, described by means of discrete element method, have been included to provide the clusters with realistic structural rigidity. The aggregates breakage process was investigated by exposing them into a well-defined shear forces, generated under both simple shear conditions and elongational flow, and by recording the time required to reach the first breakage event. Considerable attention has been given to understand the effect of electrostatic repulsive interactions and of primary particle size on both the breakage rate and cluster fragment mass distribution. The dependence on the gyration radius, on the external shear strength and on the fractal dimension has been obtained, providing a very general relationship for the breakage rate of clusters.

RESULTS: The breakage rate is exponentially decreases as the height of the energetic barrier, which two particles need to overcome in order to break a bond, increases,

$$k_b = Ae^{-BV_b} \qquad (1)$$

V_b potential barrier, A and B are fitting constants, k_b is the breakage rate of cluster.

The comparison results between simple shear and extensional flow are shown in Fig.1. The shear rate applied in simple shear has to be about 4.1 times higher than in extensional flow, which is consistent to the energy dissipation theory results.

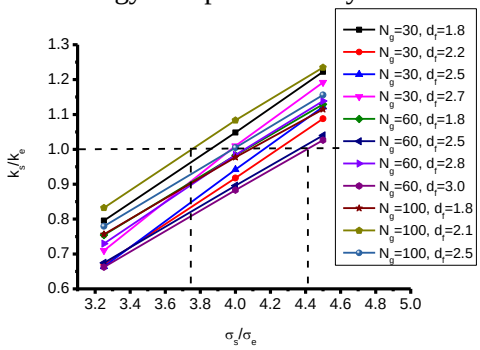

Fig. 1: Comparison between simple shear flow and extensional flow

DISCUSSION & CONCLUSIONS: The first major finding of the work is that an Arrhenius-type exponential relationship between potential barrier and the breakage rate was found to be able to satisfactorily reproduce the simulation results. The influence of all other geometrical parameters of the clusters, such as the gyration radius, the fractal dimension, the diameter of the primary particles as well as the external shear rate was also investigated, and a general correlation has been proposed for the breakage rate, with a very broad range of validity. Finally, the difference between simple shear and extensional flow on the breakage of clusters has been thoroughly analyzed using a criterion based on the energy dissipation rate. It was found that, in order to have the same breakage rate under the two different flow fields, the shear rate applied in simple shear has to be about 4.1 times higher than in extensional flow, as indicated by a simple theoretical calculation and confirmed by Stokesian Dynamics simulations.

REFERENCES: [1] Y. Harshe, M. Lattuada; **2012**; *Langmuir;* 28: 283–292.

ACKNOWLEDGEMENTS: Financial support by the Swiss National Science Foundation (grant number PP00P2133597/1) is gratefully acknowledged.

Swiss Soft Days XV

NEW SUPERANTIOXIDANT NONTOXIC SYSTEMS BASED ON CERIA

M.Spulber[1], P. Baumann[1], J. Liu[1], C.G. Palivan[1]

[1] *University of Basel, Basel, Switzerland*

INTRODUCTION: Oxidative stress induces an imbalance of reactive oxygen species (ROS), which may overwhelm cellular defences and thus cause toxicity effects. Due to the impact of oxidative stress in a variety of pathologic conditions from cancer to Parkinson's disease, Alzheimer's disease, or neurodegeneration, finding new efficient solutions to fight against oxidative stress is extremely important [1]. Ceria nanoparticles (CeNP) have been used as superantioxidant systems in various domains, ranging from material engineering to medical applications [2]. However, recent reports have indicated that CeNP lead to oxidative stress and DNA damage, and in high doses promote radical formation, via a possible Fenton-like reaction [3]. In order to reduce CeNP inherent toxicity, while preserving their unique catalytic regenerative qualities we introduce a strategy based on CeNP encapsulation in polymer nanoreactors. By encapsulation the superantioxidant activity of CeNP is preserved, whilst preventing their aggregation and interaction with H_2O_2, and decreasing their toxicity without further particle stabilization.

METHODS: Dynamic and static light scattering (DLS, SLS) were used to determine the sizes of the free CeNP and CeNP containing nanoreactors. Transmission electron microscopy (TEM) was used for characterization of the morphology of free CeNP and CeNP nanoreactors. UV-Vis spectroscopy was used to determine the conce Electron paramagnetic resonance (EPR) measurements were performed on a Bruker CW EPR Elexsys-500 spectrometer equipped with a variable temperature unit.

RESULTS: CeNP-containing nanoreactors were engineered by encapsulation of CeNP inside vesicles generated by self-assembly of PDMS-PNVP triblock copolymers under physiological pH conditions. Spin trapping EPR established that CeNP have a dual activity, involving both scavenging and generation of reactive oxygen species in the presence of hydrogen peroxide. In contrast, CeNP loaded nanoreactors benefit from polymer membrane protection, which blocks access of hydrogen peroxide to the inner cavity where CeNP are located, and therefore exhibit only an efficient scavenging activity for both hydroxyl and superoxide radicals. Upon encapsulation, the nanorectors prevent the aggregation of CeNP, and the Fenton-like reaction with hydrogen peroxide, which are known to be the main reasons for CeNP toxicity. CeNP nanoreactors were taken up by HeLa cells, and showed almost no cytotoxicity, even after long incubation times. In addition, inside nanoreactors CeNP preserved their superantioxidant activity, for both hydroxyl and superoxide radicals. Indeed, inside cells exposed to oxidative stress CeNP-containing nanoreactors were effective in ROS scavenging because of the regenerative redox chemistry of loaded CeNP. Compared to free CeNP, which induces significant cytotoxicity, CeNP-containing nanoreactors possess high superantioxidant activity, long term stability, and almost no toxicity.

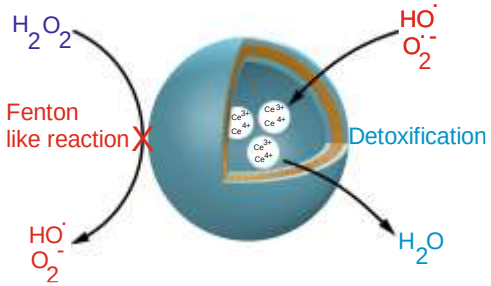

Fig. 1: Schematic representation of CeNP nanoreactors based on CeNP encapsulation inside polymer vesicles for detoxification of ROS

DISCUSSION & CONCLUSIONS: We engineered nanoreactors by encapsulation of CeNP inside polymer vesicles in order to solve their toxicity issues, by avoiding aggregation in solution and shielding them from H_2O_2, while preserving their ability to scavenge free radicals.Our strategy for engineering CeNP-containing nanoreactors represents a straightforward solution to reducing CeNP toxicity, and serving to offer the nanoreactors as an efficient solution to fighting oxidative stress.

REFERENCES: [1] M. S. Wason; **2013**; *Am. J. Transl. Res;* 5:126-131.

[2] R. C. Merrifield; **2013**; *Environ. Sci. Technol;* 47:12426-12433.

[3] E. G. Heckert; **2008**; *Environ. Sci. Technol;* 42:5014-5019.

Anisotropy of the Rheology of Strongly Interacting Ferrofluids

Aparna Sreekumari[1] and Patrick Ilg[1,2]
[1] Polymer physics, ETH Zurich, Switzerland
[2] Theory of Soft Matter, University of Reading, UK

Ferrofluids are stable colloidal suspensions of ferromagnetic nanoparticles which are stabilized against agglomeration by coating with surfactants or by surface charges. Among various properties of ferrofluids, one of the interesting properties is the change in viscosity with the orientation of an applied magnetic field, known as anisotropy of the magnetoviscous effect [1,2] whose origin needs a better understanding. Hence there is an immense interest in understanding the influence of dipolar interactions and magnetic fields on the structure and dynamics of ferrofluids. In our work we study ferrofluids modeled as magnetically hard point dipolar particles of different dipolar interaction strength using Langevin dynamics simulations. Our investigation under zero field conditions have shown an intricate correlation between the structural and dynamical properties [3]. Above a certain critical interaction strength, we find dramatic changes in micro-structures which affect the dynamics of the system. We have extended our study to understand the effect of an applied field and shear on rheological properties of ferrofluids. According to the relative orientation of magnetic field with respect to the flow, different viscosity coefficients can be defined which are known as Miesowicz viscosities [4]. We compare the Miesowicz viscosities obtained from simulations with experiments [2] and the theoretical chain model [5]. We compare our simulation results with experiments for a range of shear rates.

[1] J. P. McTague, J. Chem. Phys. 51, 133 (1969).
[2] M. Gerth-Noritzsch, D. Yu Borin, and S. Odenbach, J. Phys. Condens. Matter 23, 346002 (2011).
[3] A. Sreekumari and P. Ilg, Phys. Rev. E. 88, 042315 (2013).
[4] P. Ilg and S. Odenbach, in Colloidal Magnetic Fluids: Basics, Development and Applications of Ferrofluids, edited by S. Odenbach, Lecture Notes in Physics Vol. 763 (Springer, Berlin, 2008).
[5] A. Y. Zubarev and L. Y. Iskakova, Phys. Rev. E. 61, 5415 (2000).

In-situ characterization of the wetting behaviour of individual particles at liquid-liquid interfaces

M.Zanini[1], L. Isa[1]

[1] ETH Zürich, Zürich, Switzerland.

INTRODUCTION: Particles at fluid interfaces have been investigated intensively in the past decades and nowadays are becoming an important topic in colloid science. They are related to a variety of technological applications spanning from delivery [1], to emulsion stabilization [2] for cosmetics and food science purposes.

Particle position relative to the fluid interface depends on several factors such as chemical nature, size, geometrical roughness and wettability [3]. The latter is the key parameter, which directly determines the contact angle θ of the particle at the interface. In brief, θ defines the structural, dynamical and thermodynamical properties of particle adsorption and self-assembly at fluid interfaces.

METHODS: In this work we present a method based on freeze-fracture shadow-casting combined with cryo-SEM (FreSCa cryo-SEM) imaging of the oil/water interface.

RESULTS: FreSCa cryo-SEM is suitable not only for hard spheres [4] but also for soft hydrogels [5] and Janus particles [6]. Moreover, it allows direct investigation of the role of surface roughness in wetting of colloids at interfaces.

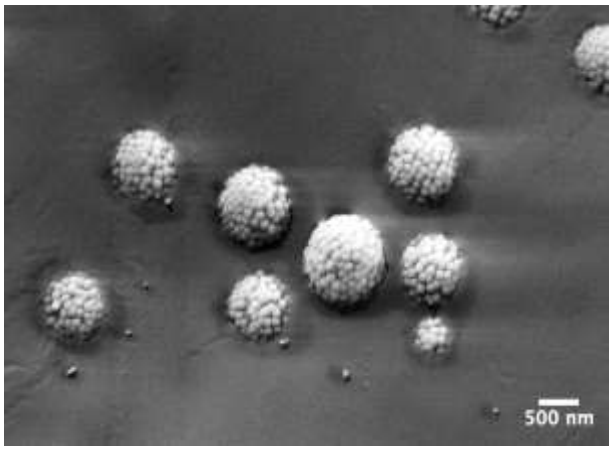

Fig. 1: FreSca Cryo-SEM image of roughened particles at water/oil

DISCUSSION & CONCLUSIONS: FreSCa cryo-SEM is a novel, powerful and reliable tool for the wetting characterization of both hydrophilic and hydrophobic hard spheres, soft objects and also colloids with shape and chemical anisotropies at water/oil interfaces. It represents a well-established method able to tackle the requirements for the future challenges regarding colloids wetting behaviour at liquid-liquid interfaces.

REFERENCES:

[1] Verma A., Stellacci F., Small, 6, 12-21 (2010).

[2] San-Miguel A., Behrens S. H., Langmuir, 28, 12038-12043 (2012).

[3] Maestro A., Guzmán E., Ortega F., Rubio R. G., Current Opinion in Colloid & Interface Science (2014), "article in press".

[4] Isa L., Lucas F., Wepf R., Reimhult E., Nat Commun, 2, 438 (2011).

[5] Geisel K., Isa L., Richtering W., Angewandte Chemie International Edition, 126, 5005-5009 (2014).

[6] Alla Synytska, M. Sc Alina Kirillova, and Lucio Isa, ChemPlusChem, 79, 656-661 (2014).

ACKNOWLEDGEMENTS: Many thanks to the group of Complex Materials and the SCOPEM centre for access and training to the electronic microscopes, to the entire LSST-ISA group for the nice and fruitful working atmosphere.

Depletion-Induced Closed-Loop of Isotropic-Nematic Coexistence in Amyloid Fibrils and Polymer Solutions

Jianguo Zhao, Chaoxu Li, Raffaele Mezzenga
Food and Soft Materials Laboratory, ETH Zürich, Switzerland

INTRODUCTION: High-aspect-ratio amyloid fibrils exhibit an isotropic-nematic (I-N) phase transition above critical concentration [1]. Yet, the I+N coexistence expected theoretically in rod-like colloids, remains elusive in amyloid fibrils suspensions, probably due to the extremely weak I-N interfacial tension and low enthalpy of transition [2]. We study solutions of non-adsorbing polymers and amyloid fibrils, and report -for the first time- an unusual closed-loop of I+N coexistence. We combine depletion potentials in dilute and semi-dilute polymer regime with DLVO theory and the principle of equivalent law of corresponding states to calculate variations of the second virial coefficient and rationalize the phase behavior.

METHODS: Amyloid fibrils were prepared by incubating 2 wt. % β-lactoglobulin protein at pH 2 and 90 °C for 5h. Dextran, was used as the depletion agent. At constant ionic strength and pH 2, the mixture of amyloid fibrils and Dextran was incubated for 2 days to reach equilibrium.

RESULTS: As a general, surprising observation, one can note that, when the Dextran concentration greatly exceeds overlap concentration ($c^*_{polymer}$), the I+N biphasic region tends in all cases to weaken and eventually disappears in a closed-loop re-entrant phase behavior (fig. 1). The biphasic region appears to dilate on increasing ionic strength (mM), e.g. from 75 to 100 [fig. 1 (b)] and molecular weight of Dextran, e.g. from 70 000 to 150 000 [fig. 1(c)], in agreement with expected increased attractive potential in both cases.

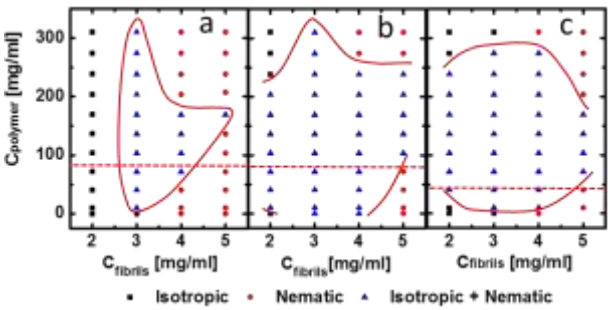

Fig. 1: Effect of ionic strength and molecular weight of polymer on phase diagram. (a) M_w: 70 000, ionic strength: 75; (b) M_w: 70 000, ionic strength: 100; (c) M_w: 150 000, ionic strength: 75. $c^*_{polymer}$ are indicated as dotted lines.

DISCUSSION & CONCLUSIONS:
We calculate the evolution of the depletion potential as a function of Dextran concentration, and the total potential including DLVO and the depletion interactions (fig. 2).

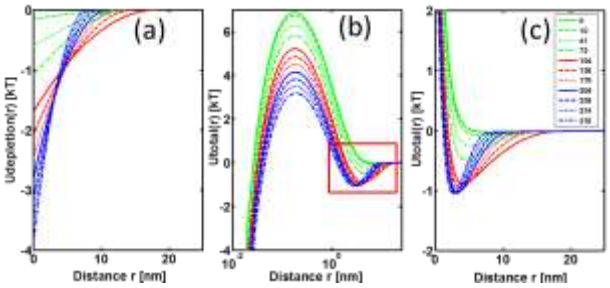

Fig. 2: Interaction potentials for amyloid fibrils at varying concentrations (mg/ml) of Dextran (M_w: 70 000) and 75 mM ionic strength.

The changes of the reduced second virial coefficient ΔB_2^* ($\Delta B_2^* = B_2^*_{(DLVO+Depletion)} - B_2^*_{DLVO}$) as a function of polymer concentration (fig. 3), correlates perfectly with the closed-loop phase behavior shown in fig. 1.

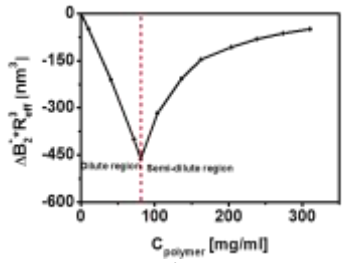

Fig. 3: Evolution of ΔB_2^* as a function of polymer concentration.

In conclusion, a closed-loop of I+N coexistence was observed using amyloid fibrils in presence of a non-absorbing polymer. By modelling interactions among fibrils, we show how this phase behavior can be interpreted by the non-monotonic evolution of the reduced second virial coefficient.

REFERENCES: [1] J. M. Jung and R. Mezzenga; **2010**; *Langmuir;* 26: 504-514.[2] S. J. Mills and D. J. Cleaver; **2000**; *Mol. Phys.;* 98, 1379-1389.

ACKNOWLEDGEMENTS: J. Z. wishes to thank China Scholarship Council for financial support.